

ITCZ Dynamics and Hadley Circulation

B. N. Goswami

SERB Distinguished Fellow

Cotton University, Guwahati

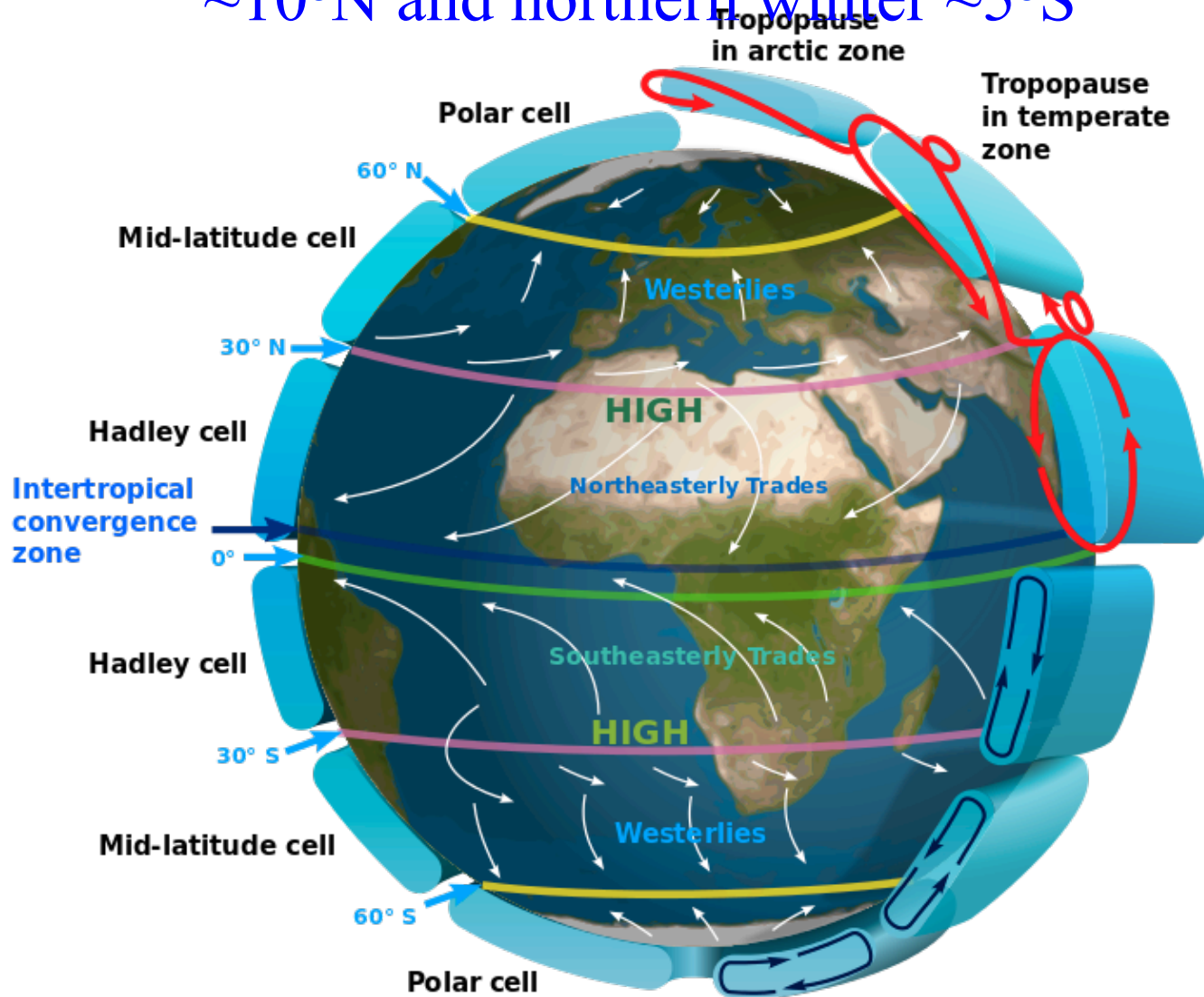
21 May, 2022

Why ITCZ Dynamics is Important for Understanding Indian Monsoon Rainfall?

Recall:

- **Indian monsoon is a manifestation of seasonal migration of the ITCZ during northern summer.**
 - **Indian monsoon rainfall → ITCZ rainfall**
 - **Large-scale** part of ITCZ is governed by large-scale convergence and ascending motion of the global ITCZ
 - The **small-scale** part of monsoon ITCZ is controlled by regional factors like land-ocean contrast, orography etc.
- Today's lecture: What maintains the large scale global ITCZ?

Recall that low level winds over tropics tends to converge to a location known as the ITCZ producing ascending motion. On annual mean, it happens around 6°N , in northern summer $\sim 10^{\circ}\text{N}$ and northern winter $\sim 5^{\circ}\text{S}$

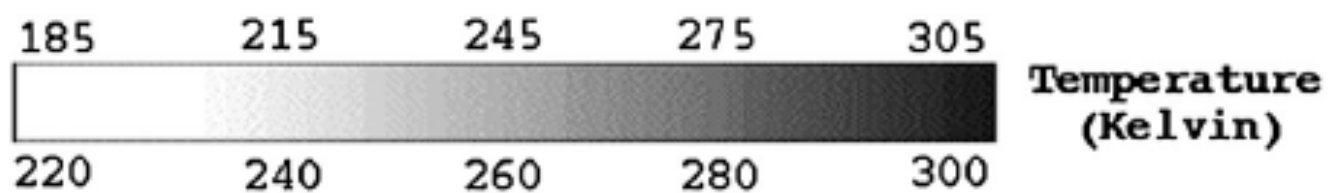
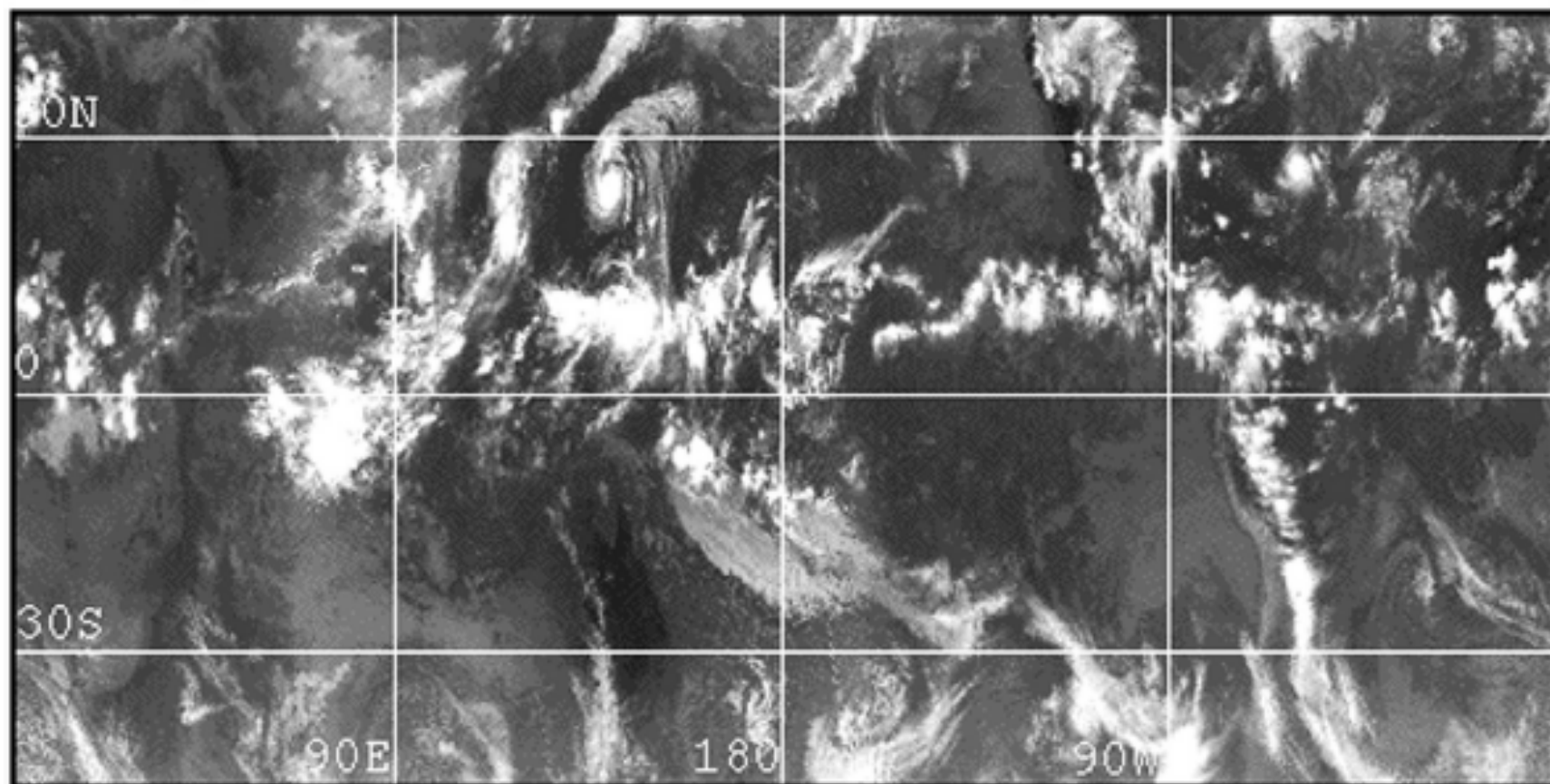


The ITCZ has very large zonal scale and could be seen in **monthly mean cloud pictures** with some inhomogeneity.

The ascending motion is the ascending branch of the Hadley cell. Thus ITCZ and Hadley cell are synonymous.

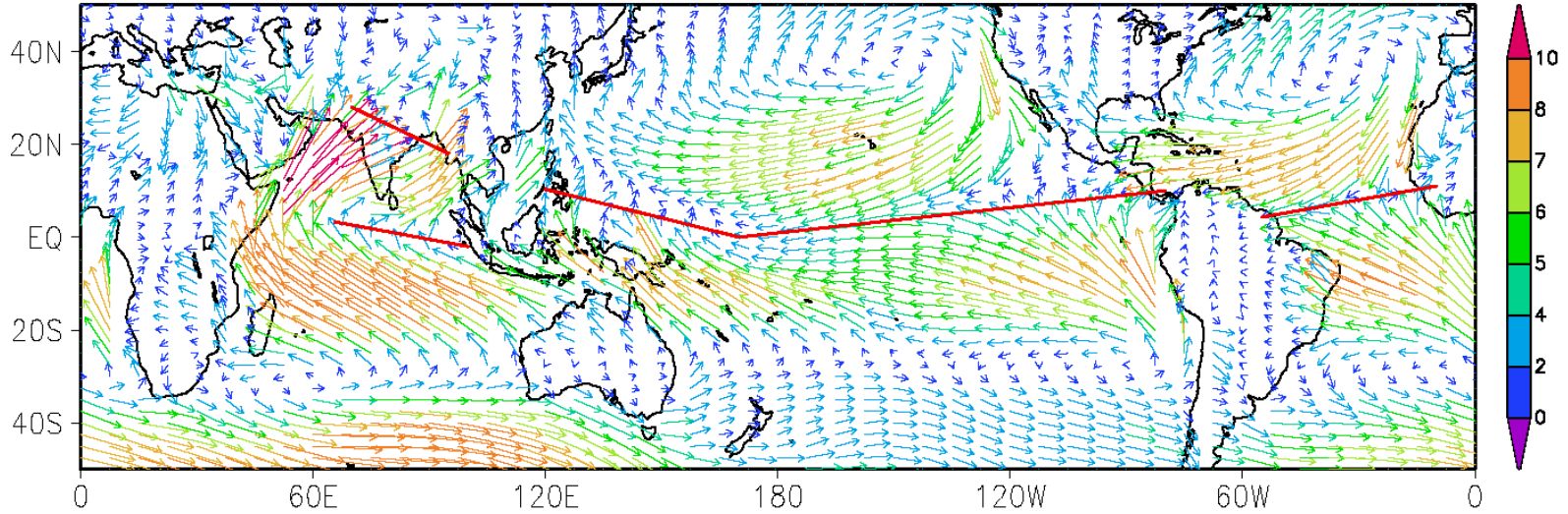


(a) 7 September 1991

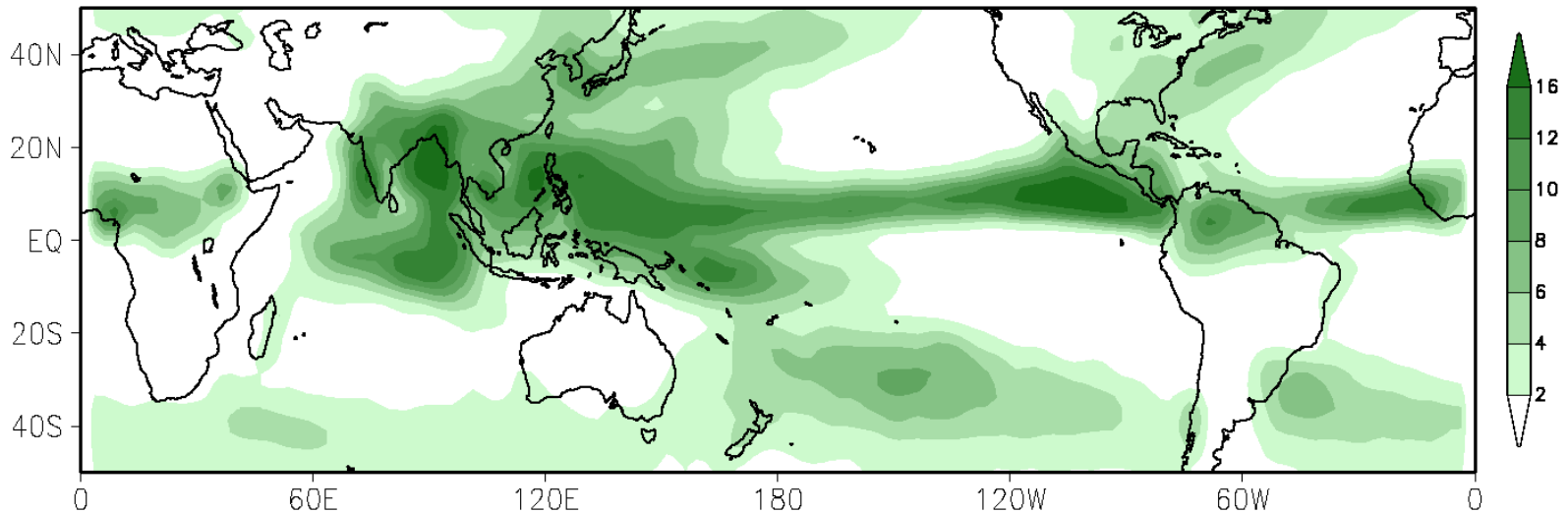


Although ITCZ is largely zonal, there are some inhomogeneity as seen below

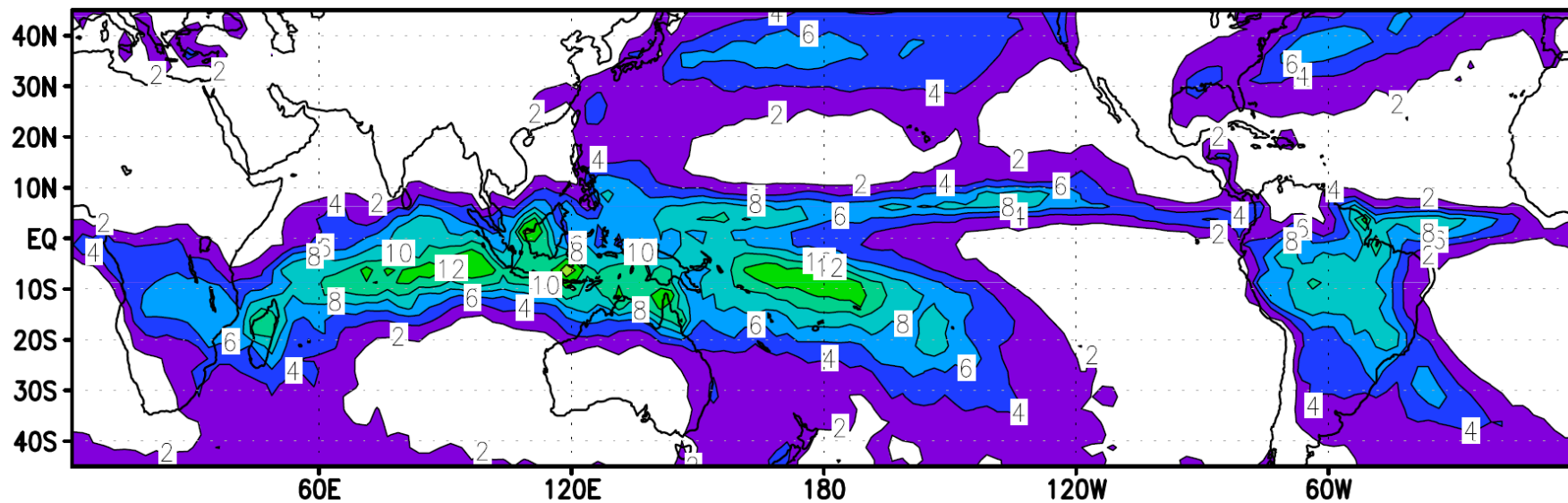
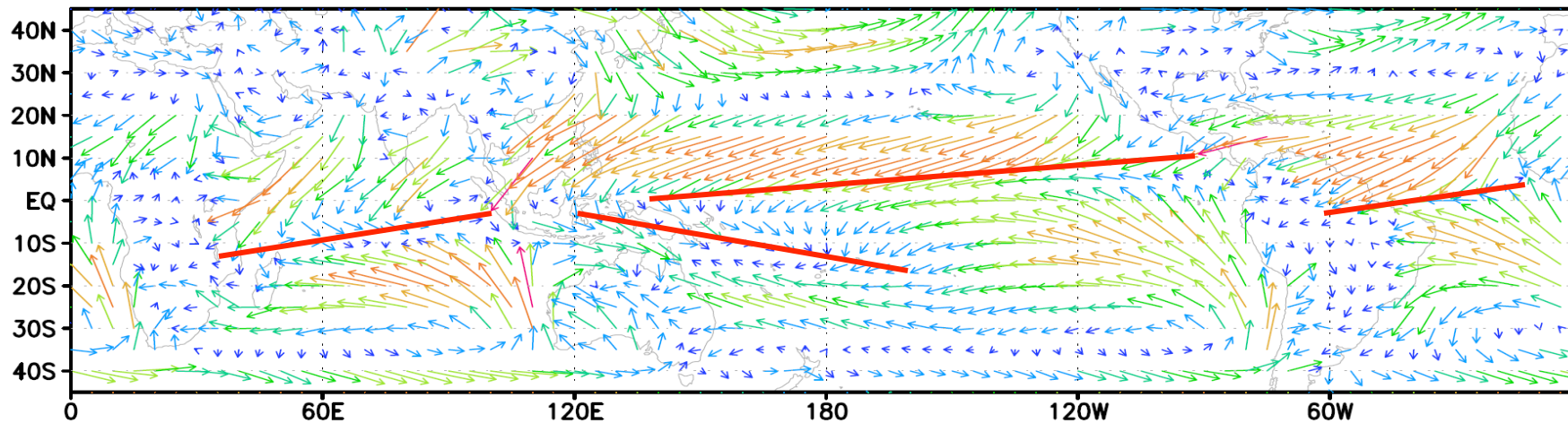
Surface Wind Climatology of July (ms^{-1})



Rainfall Climatology of July (mmday^{-1})



Mean January rainfall and surface wind convergence



Climatological Annual variation of the ITCZ (Rain band)

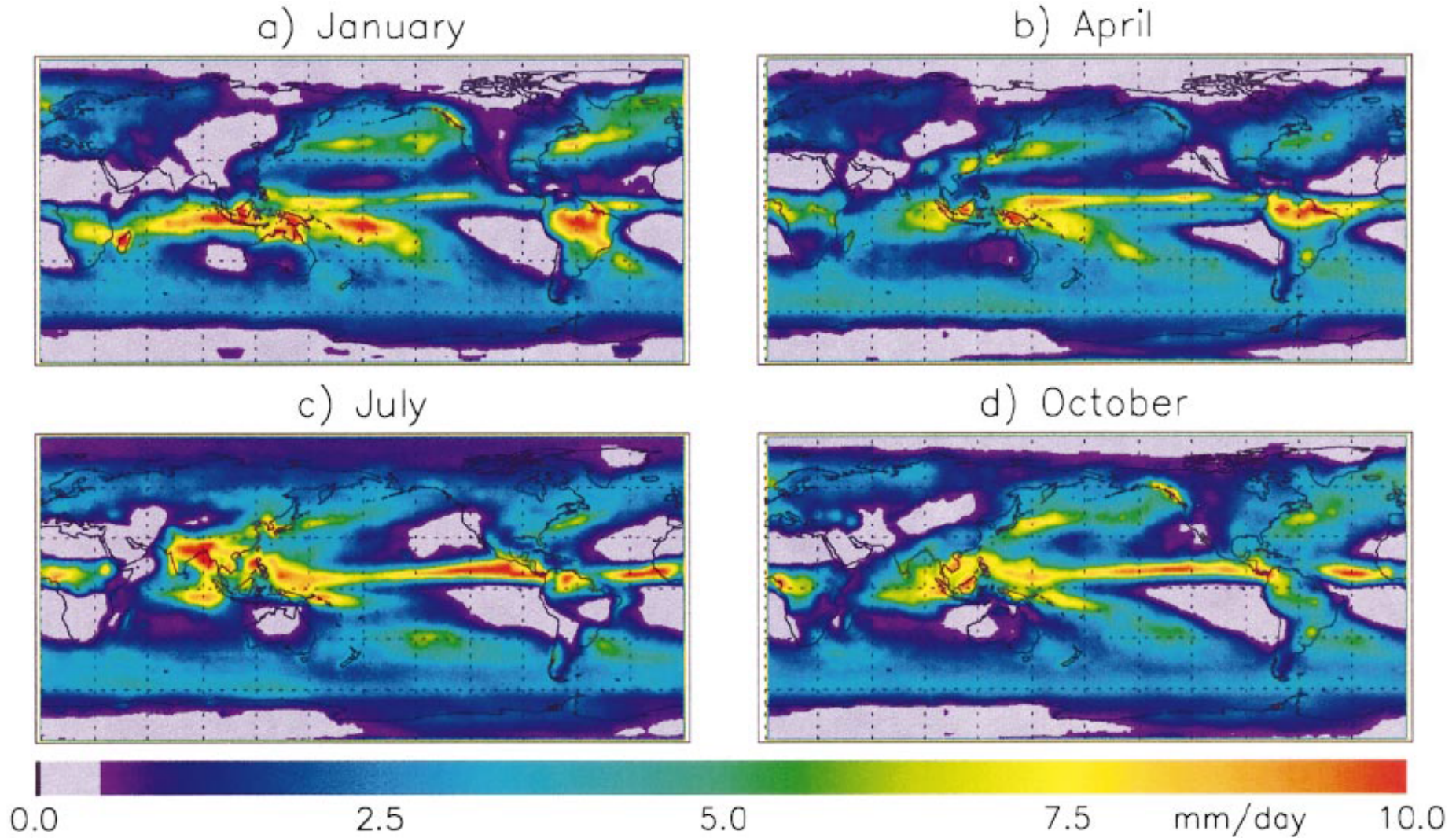


FIG. 9. The 23-yr (1979–2001) seasonal mean precipitation (mm day^{-1}) for (a) Jan, (b) Apr, (c) Jul, and (d) Oct.

Zonal Mean Precipitation

1979–2001 Climatology

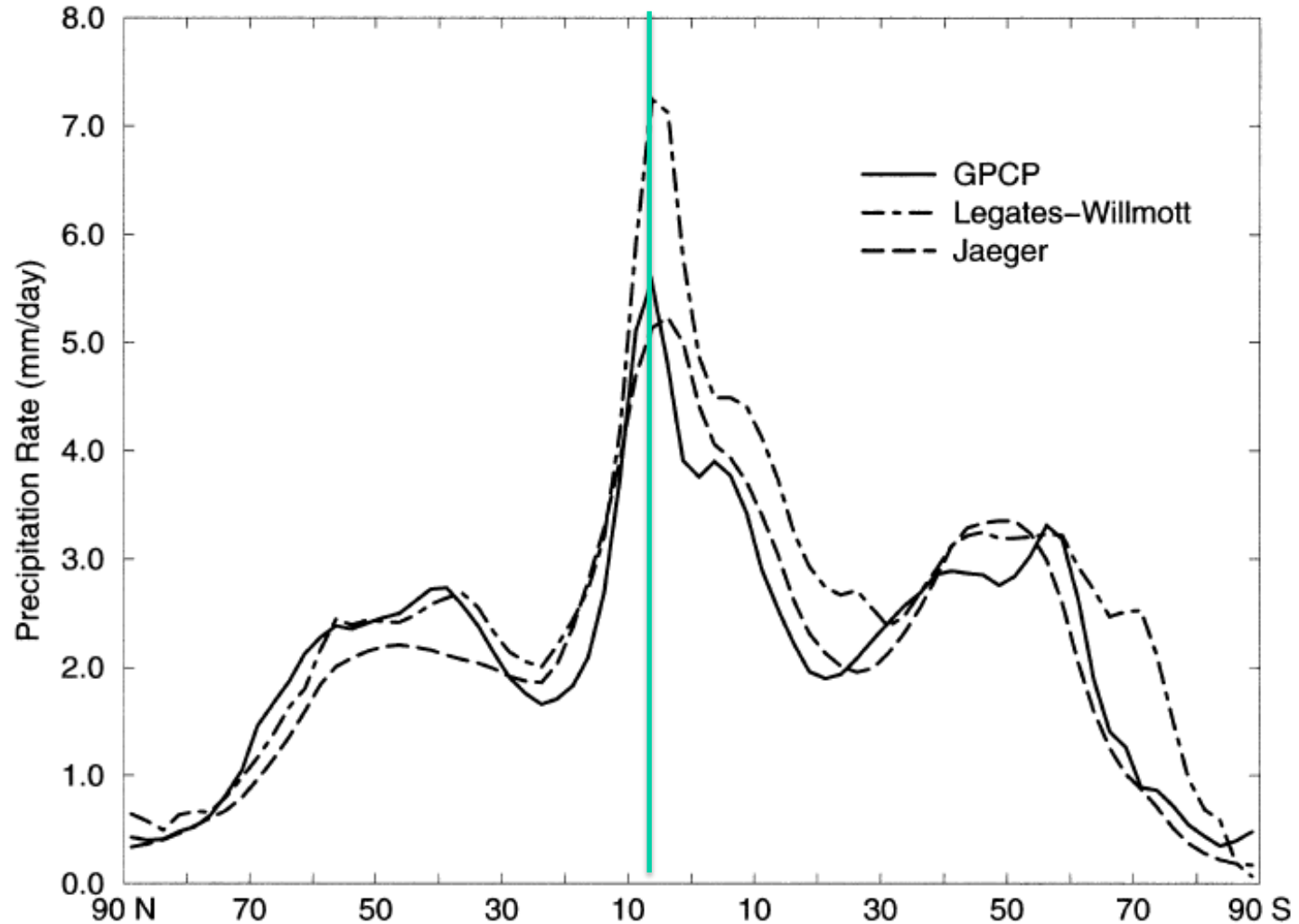


FIG. 5. Zonally averaged annual mean climatologies of precipitation (mm day^{-1}): the GPCP (solid line, see Fig. 4), Legates and Willmott (1990) (dot-dashed line), and Jaeger (1976) (long-dashed line).

Adler et al., 2003: v.2-GPCP, J. Hydrology, 4, 1147

Waliser and Gautier, 1993:
A satellite derived
climatology of the ITCZ, *J.
Climate*, 6, 2162- 2174

Highly reflective clouds
(HRC) created from daily
visible and infrared
mosaics, analysed into 1°
 $\times 1^\circ$ grids between
January, 1971 and
December 1987.

→ No. of days such HRC
occurs in a grid box per
month.

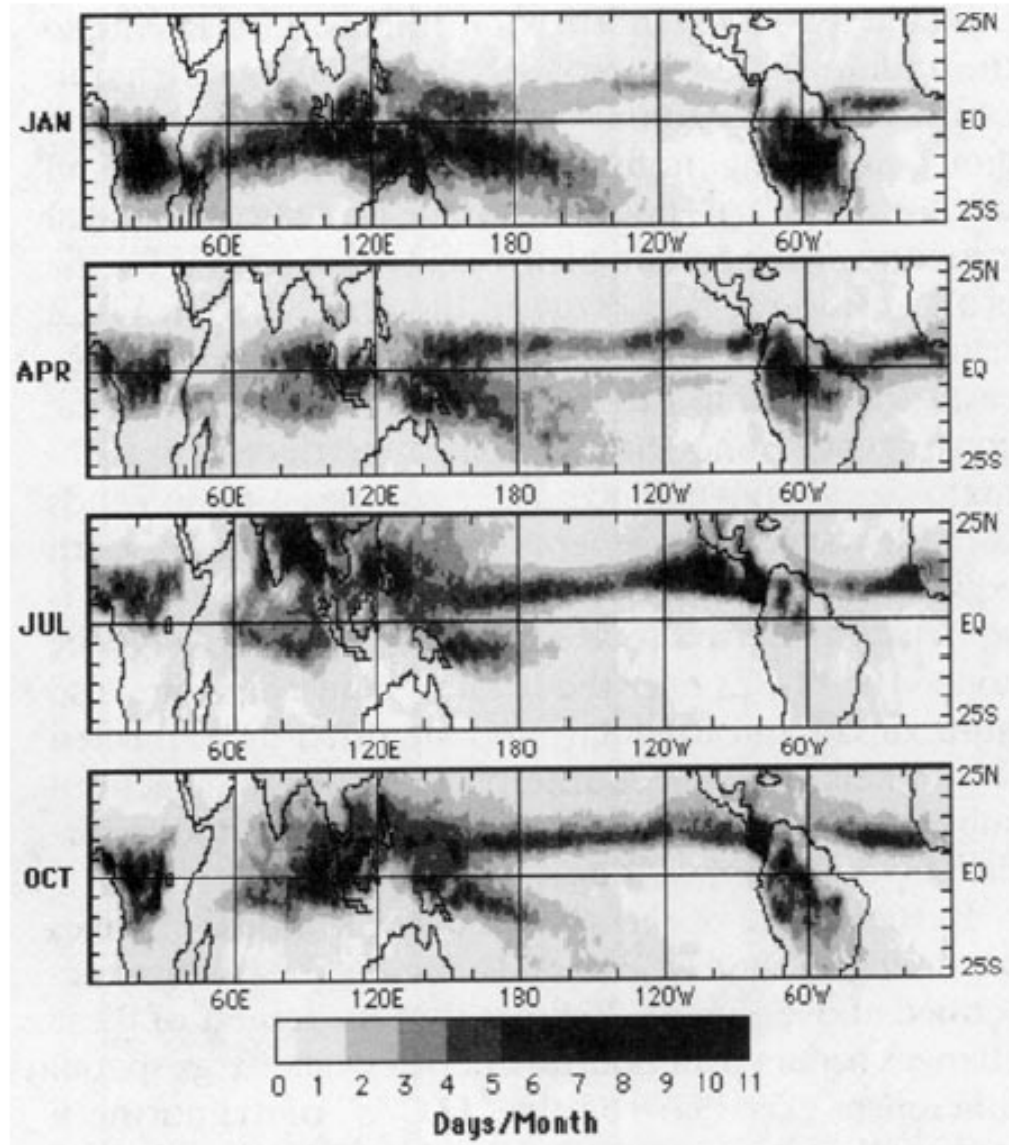


FIG. 1. Mean monthly "ITCZ" structure for the months: (a) January, (b) April, (c) July, and (d) October. These mean monthly images were computed from 17 years of monthly HRC data. Values represent the number of days per month (sampled once per day) the given grid point was covered by a large-scale deep convective system (subjectively determined; see section 2).

Meridional Migration of the ITCZ

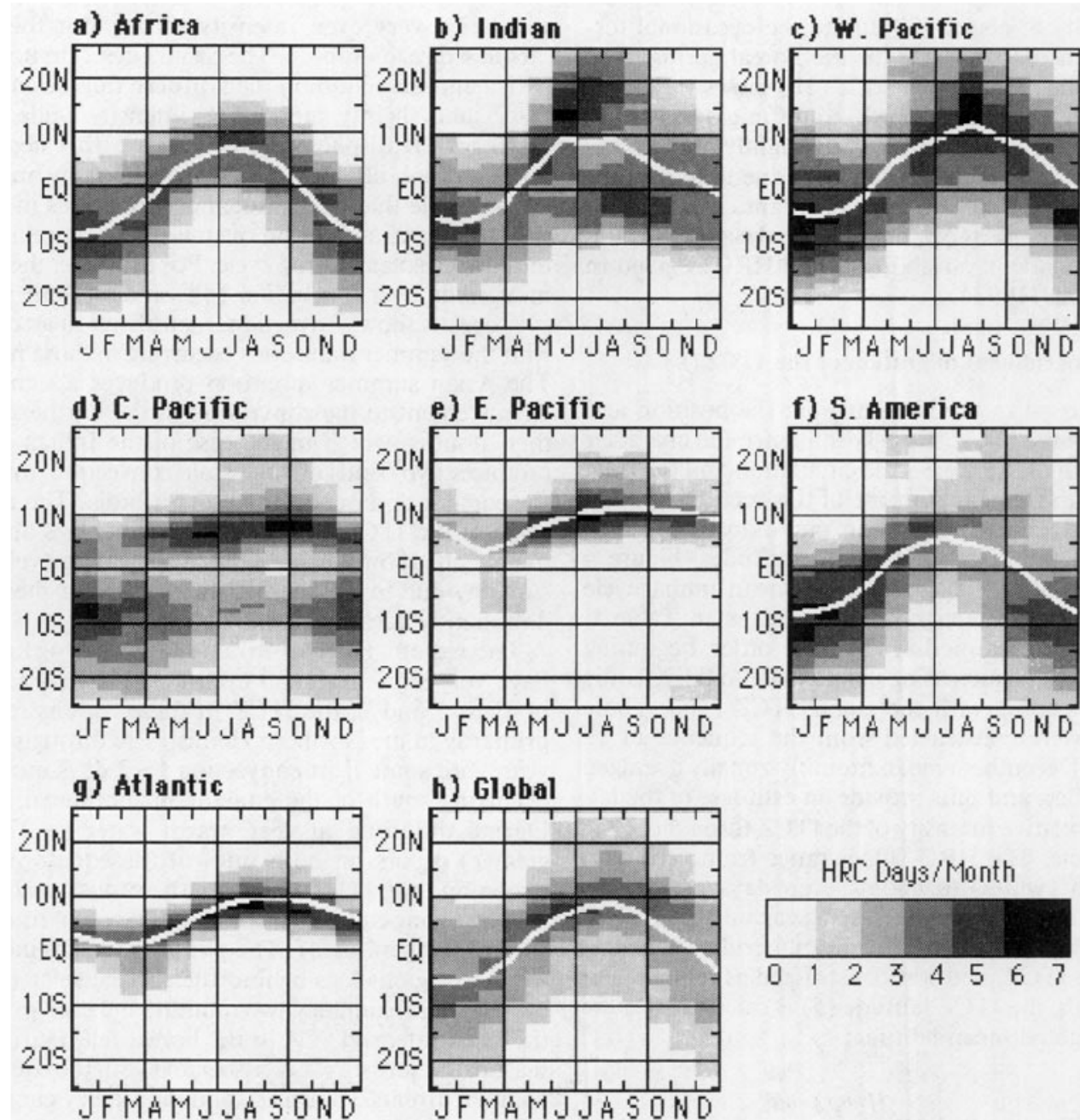
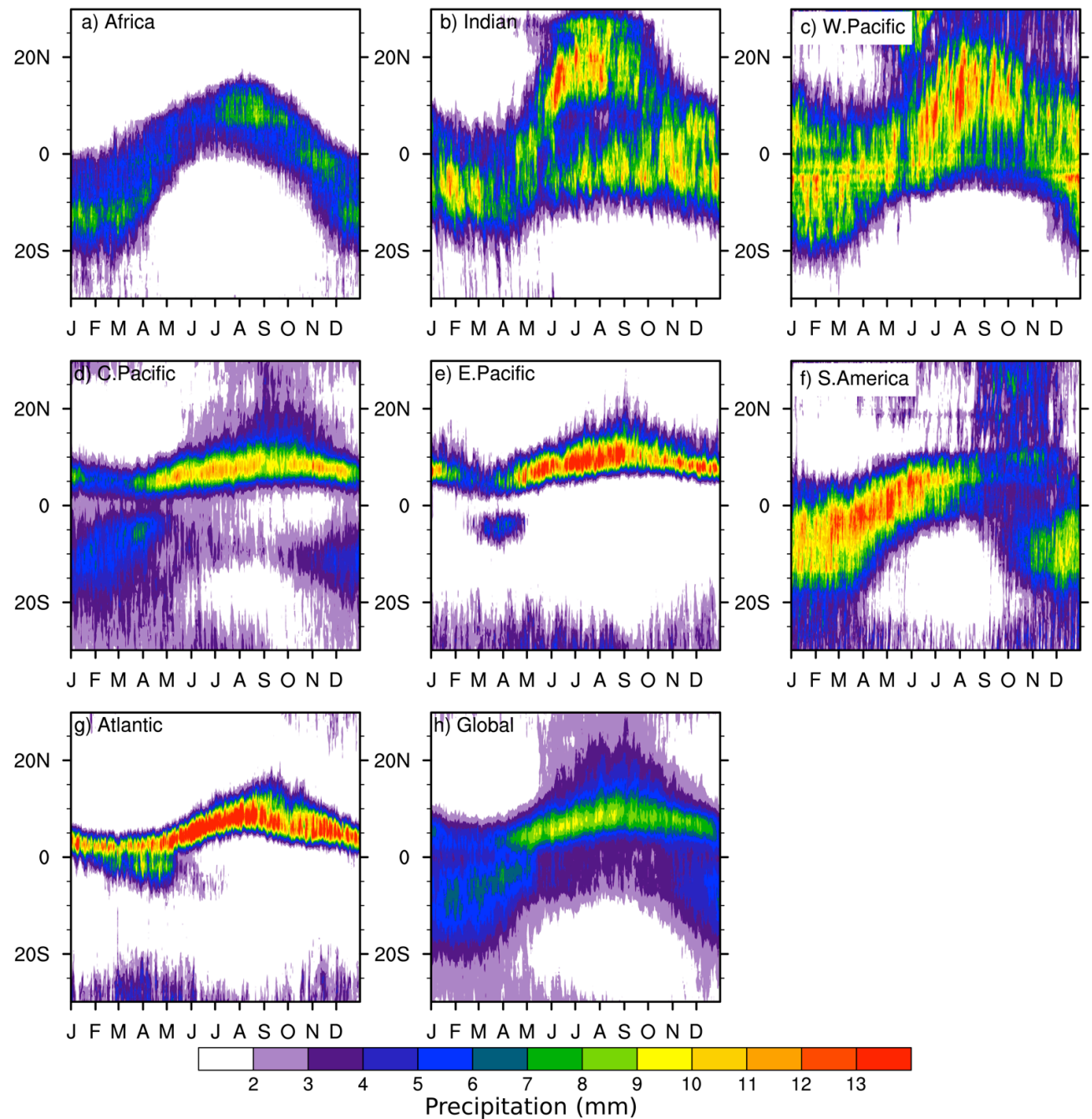


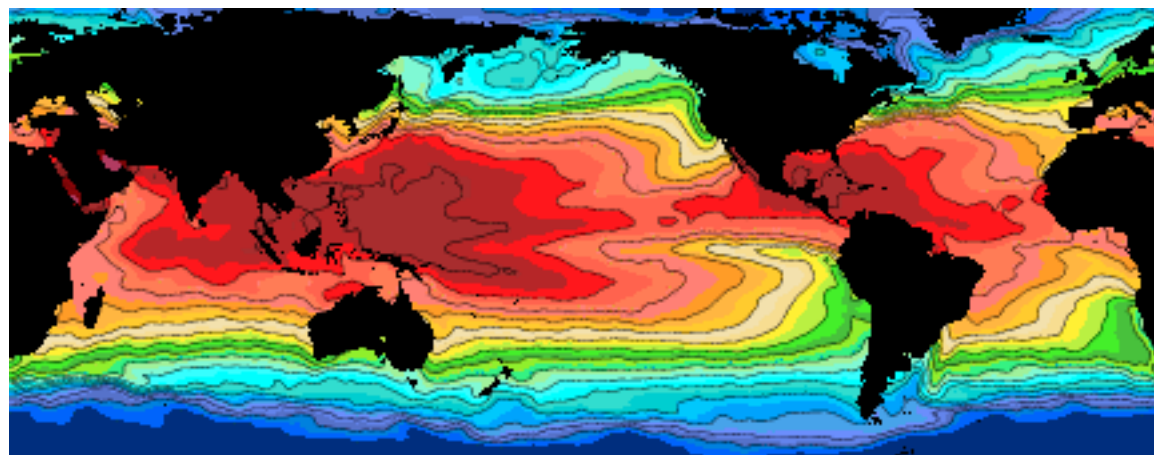
FIG. 4. Time-latitude diagrams of the annual cycle of ITCZ migration for the eight regions specified in Table 1. Annual cycles were computed from the 17 years of HRC data. White lines are quantitative estimates of the mean monthly ITCZ position (except central Pacific region); see text for computation.

- Today, better data is available. Can we construct the meridional structure and association with SST with rainfall data?
- For this, you may take daily TRMM 3B42 rainfall data (1998- 2019). Create monthly means. And plot the long term mean at different latitudes like in slide 13 over Indian Ocean, western Pacific, central Pacific and east Pacific

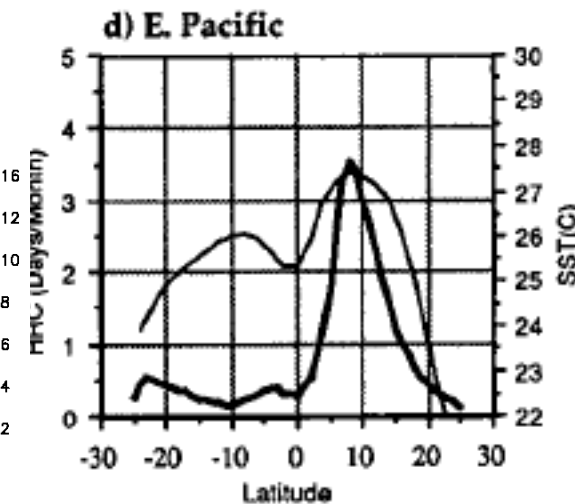
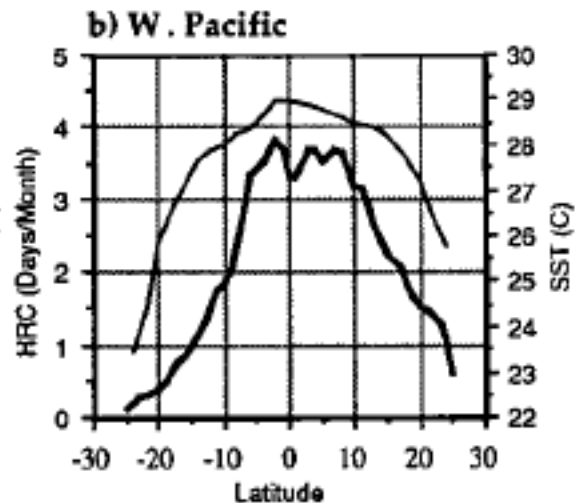
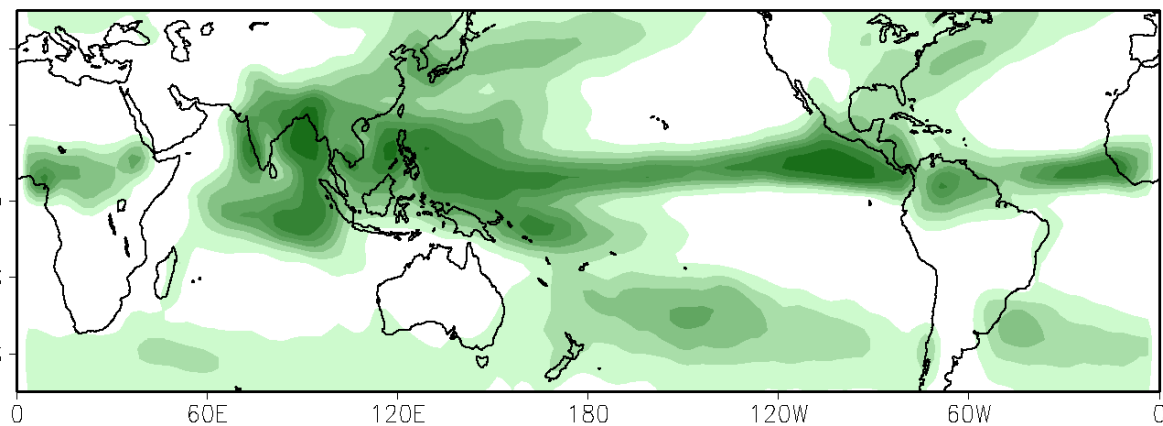
Similar to the Waliser and Gautier work, northward migration of the ITCZ from daily TRMM data over different sectors.



Why the mean ITCZ location also tends to be location of the zonal mean SST maximum?



Rainfall Climatology of July (mmday^{-1})



Lindzen R S and S. Nigam, 1987: On the Role of Sea Surface Temperature Gradients in Forcing Low-Level Winds and Convergence in the Tropics, J. Atmos. Sci., 44, 2418-

SST with a zonal Maximum leads to a Low pressure at SST maximum



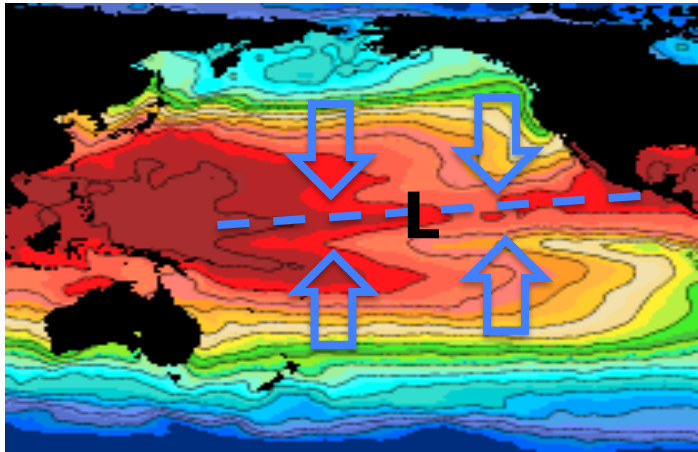
SST with a zonal Maximum leads to a Low pressure at SST maximum leading to



Convergent winds to the location of SST maximum
→ moisture convergence and uplift



Organized convection, rainfall and the ITCZ



What drives the ITCZ & Hadley Circulation?

- ◆ Hadley circulation is thermally direct, +heat input in tropics (ascent) → -ve heat input polar region (descent)
→ Resultant motion is Angular momentum conserving, thermally forced
- ◆ But the ITCZ is a region of intense convection → large ascending motion → Modified by latent heating in tropics

Other Questions:

- On annual mean sense, the ITCZ is located at $\sim 6^\circ\text{N}$. **What determines the location of the ITCZ?**
- Width of the ascending branch of the Hadley circulation is much narrower than that of the descending branch. What determines it and how do we define the **'intensity'** and **'width'** of the Hadley circulation?

It is determined by the angular momentum conserving flow forced by the heating gradients, thermal plus latent heating. Foundation for Hadley circulation dynamics was set by the following pioneering studies,

Schneider, E and R. Lindzen, 1977: Axially symmetric steady state models of the basic state for Instability and climate studies, Part-I, Linearized calculations, J. Atms.Sci. 34,263

Schneider, E, 1977: Axially symmetric steady state models of the basic state for Instability and climate studies, Part-II, Nonlinear calculations, J. Atms.Sci. 34,280

Held I. M. and A. Y, Hao, 1980: Nonlinear axially symmetric circulation in a nearly inviscid atmosphere, J. Atmos. Sci., 37, 515

Held and Hou, 1980, JAS, 37.3 (1980): 515-533

The Model Equations: Axisymmetric, nearly inviscid

We consider the primitive equations for a dry Boussinesq fluid on a hemisphere, confined between the surface and a rigid lid at height H above the surface. The flow is forced by radiative heating proportional to the difference between the fluid temperature and a specified “radiative equilibrium” temperature. Linear vertical diffusion of heat and momentum (with Prandtl number unity, unless otherwise noted) is the only small-scale mixing in the fluid interior. The diffusivity is chosen to be a constant, independent of height and latitude. A zero stress boundary condition is imposed at the top surface, and the stress at the ground is taken to be proportional to surface wind. Zero vertical heat flux is imposed at both upper and lower boundaries.

Steady State equations are

$$\left. \begin{aligned}
 0 &= -\nabla \cdot (\mathbf{v}u) + fv + \frac{uv \tan\theta}{a} + \frac{\partial}{\partial z} \left(\nu \frac{\partial u}{\partial z} \right) \\
 0 &= -\nabla \cdot (\mathbf{v}v) - fu - \frac{u^2 \tan\theta}{a} - \frac{1}{a} \frac{\partial \Phi}{\partial \theta} \\
 &\quad + \frac{\partial}{\partial z} \left(\nu \frac{\partial v}{\partial z} \right) \\
 0 &= -\nabla \cdot (\mathbf{v}\Theta) - (\Theta - \Theta_E) \tau^{-1} + \frac{\partial}{\partial z} \left(\nu \frac{\partial \Theta}{\partial z} \right) \\
 0 &= -\nabla \cdot \mathbf{v} \\
 \frac{\partial \Phi}{\partial z} &= g \Theta / \Theta_0
 \end{aligned} \right\} \text{Forcing}, \quad (1)$$

with boundary conditions

$$\left. \begin{aligned} \text{at } z = H: \quad w = 0; \quad \frac{\partial u}{\partial z} = \frac{\partial v}{\partial z} = \frac{\partial \Theta}{\partial z} = 0 \\ \text{at } z = 0: \quad w = 0; \quad \frac{\partial \Theta}{\partial z} = 0; \\ \nu \frac{\partial u}{\partial z} = Cu; \quad \nu \frac{\partial v}{\partial z} = Cv \end{aligned} \right\} \quad (1a)$$

Here $\mathbf{v} = (v, w)$ is the velocity and $\nabla = [(a \cos \theta)^{-1} \times \partial(\cos \theta) / \partial \theta, \partial / \partial z]$ the gradient operator in the meridional-vertical plane. τ is a constant radiative damping time, and C a constant drag coefficient. $g\Theta / \Theta_0$ is the buoyancy in the Boussinesq approximation. The notation is otherwise standard. Θ_E is given the form

$$\frac{\Theta_E(\theta, z)}{\Theta_0} = 1 - \frac{2}{3} \Delta_H P_2(\sin \theta) + \Delta_v \left(\frac{z}{H} - \frac{1}{2} \right), \quad (2)$$

where Θ_0 is the global mean of Θ_E , Δ_H and Δ_v are both nondimensional constants, and P_2 is the second Legendre polynomial $P_2(x) = \frac{1}{2}(3x^2 - 1)$. Δ_H and Δ_v are, respectively, the fractional change in potential temperature from equator to pole and from the top to the bottom of the fluid in radiative equilibrium.

Radiative equilibrium θ

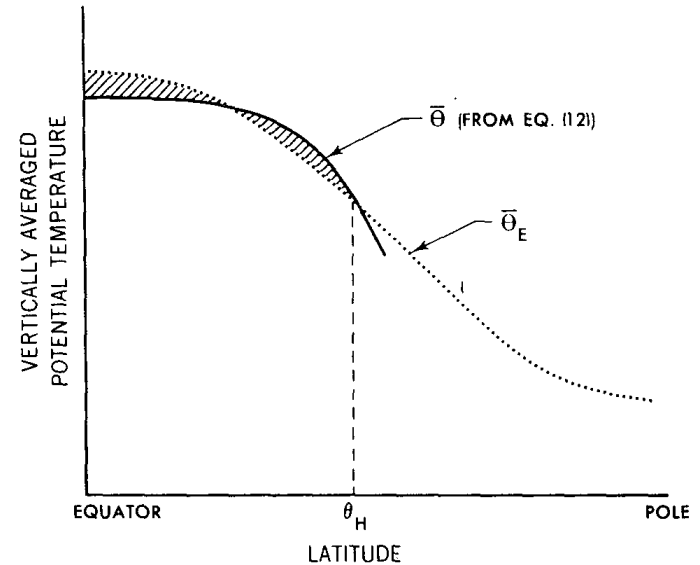
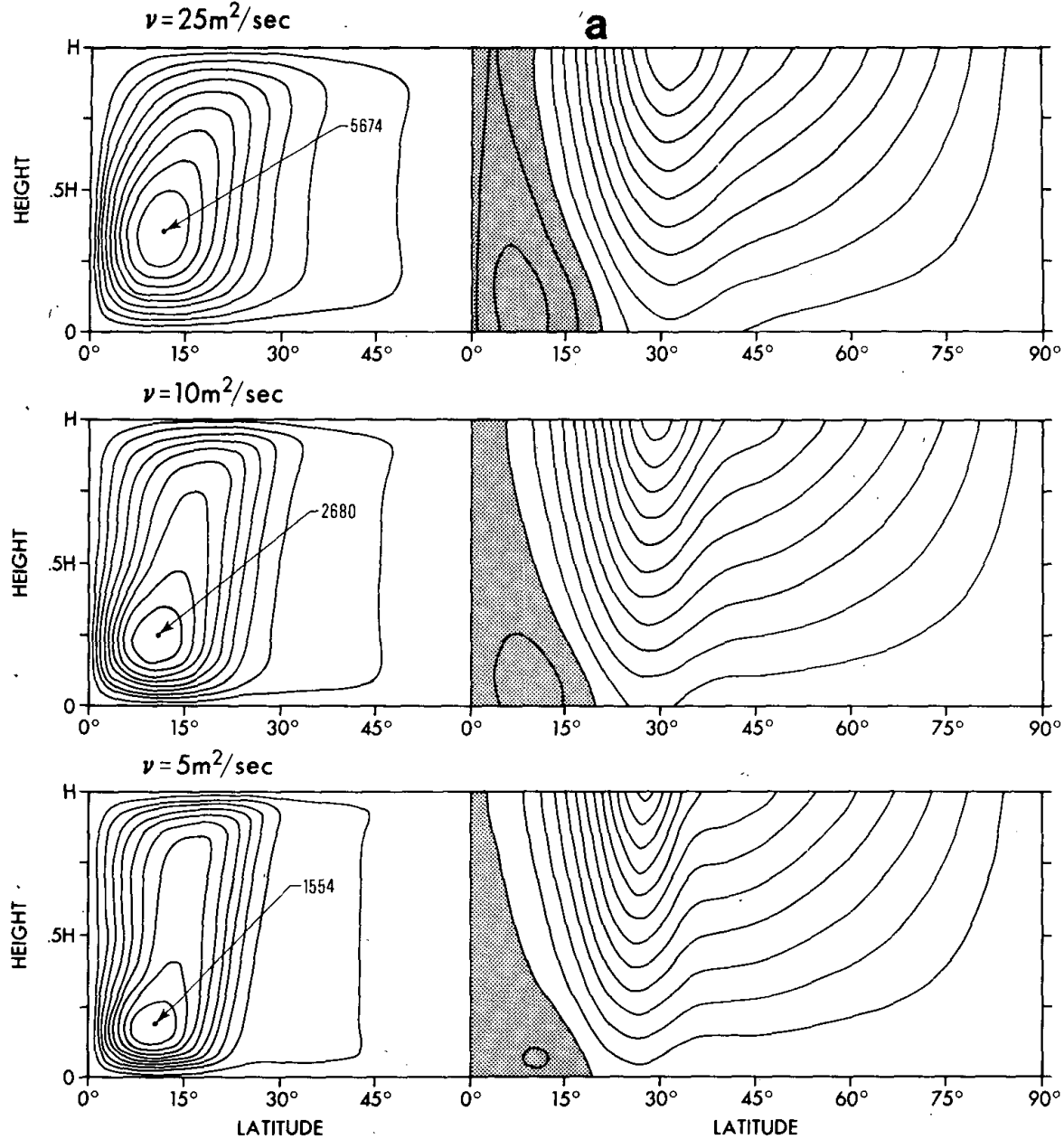
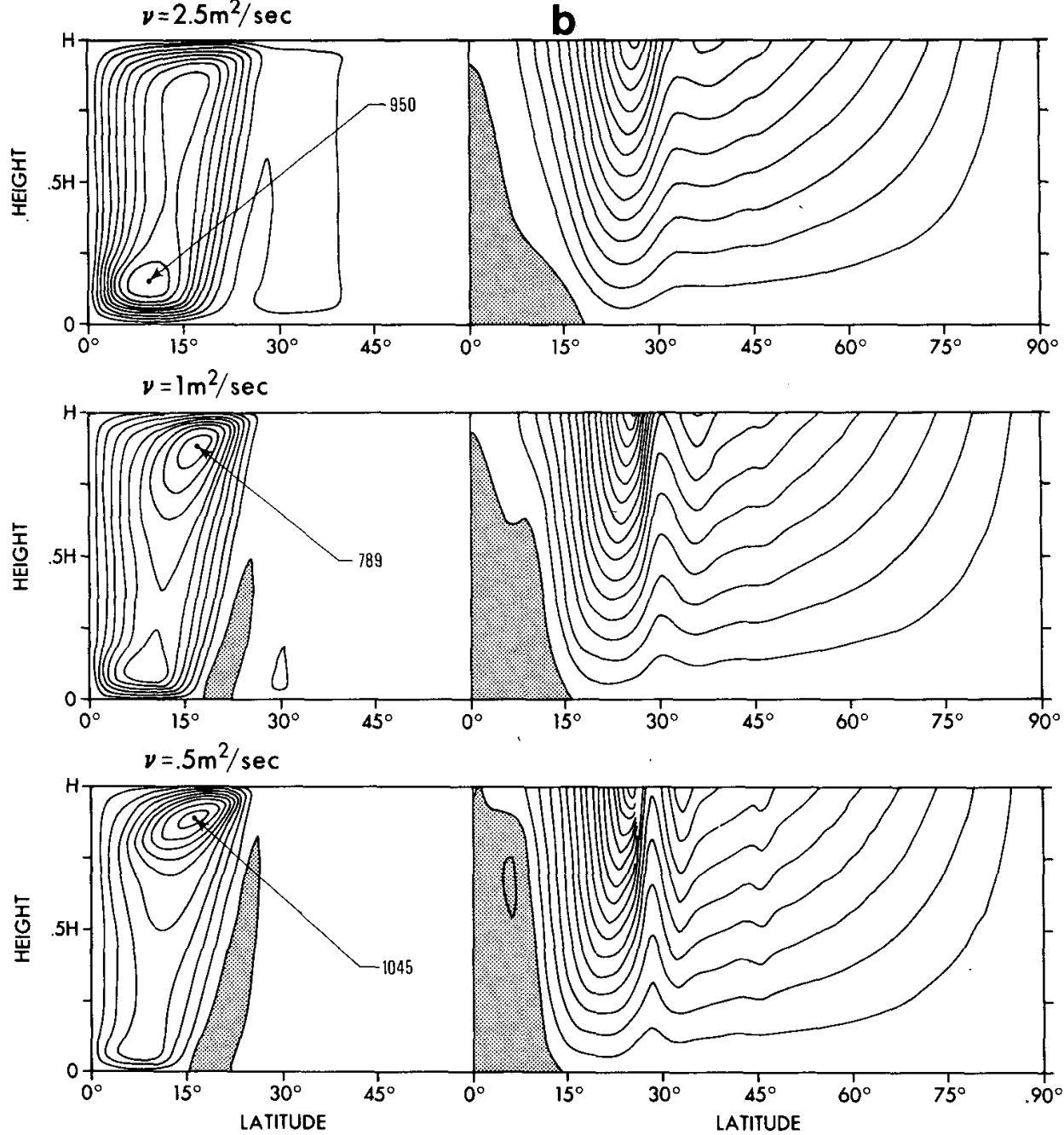


FIG. 1. The equal-area geometric construction equivalent to the argument of Section 4a. The two shaded areas are equal.



Decreasing
Viscosity ν

FIG. 4a. Calculated meridional streamfunctions and zonal wind fields in the standard case. In the left part of the figure, the streamfunction ψ is given for $\nu = 25, 10$ and $5 \text{ m}^2 \text{ s}^{-1}$, with a contour interval of $0.1 \psi_{\text{max}}$. The value of ψ_{max} ($\text{m}^2 \text{ s}^{-1}$) is marked by a pointer. The right part of each figure is the corresponding zonal wind field, with contour intervals of 5 m s^{-1} . The shaded area indicates the region of easterlies.



Decreasing
Viscosity ν

FIG. 4b. Calculated meridional streamfunctions and zonal wind fields as described in Fig. 4a. The shaded region in the ψ field corresponds to a Ferrel cell, $\psi < 0$.

Width of the Hadley Cell

This momentum conserving flow clearly cannot continue to the pole. It is assumed, therefore, that it continues only up to some latitude θ_H . Poleward of θ_H the meridional circulation is assumed to be identically zero, so that $\Theta = \Theta_E$ and $u = u_E$. θ_H can be determined by requiring continuity of temperature at $\theta = \theta_H$ and assuming a balanced zonal wind:

$$fu + \frac{u^2 \tan\theta}{a} = - \frac{1}{a} \frac{\partial\Phi}{\partial\theta}$$

Evaluating this expression at $z = 0$ and $z = H$, and using the vertically integrated hydrostatic equation,

Leads to...

$$\frac{1}{3}(4R - 1)y_H^3 - \frac{y_H^5}{1 - y_H^2} - y_H + \frac{1}{2} \ln\left(\frac{1 + y_H}{1 - y_H}\right) = 0 \quad (17)$$

for $y_H \equiv \sin\theta_H$. The solution to this equation as a function of R is compared with the small-angle approximation $(\frac{5}{3}R)^{1/2}$ in Fig. 2.

Where,

$$R = \frac{gH\Delta_H}{\Omega^2 a^2} \quad (6)$$

If $R \ll 1$, then $u_E/\Omega a \approx R \cos(\theta)z/H$. In this limit R can be thought of as a thermal Rossby number. Note

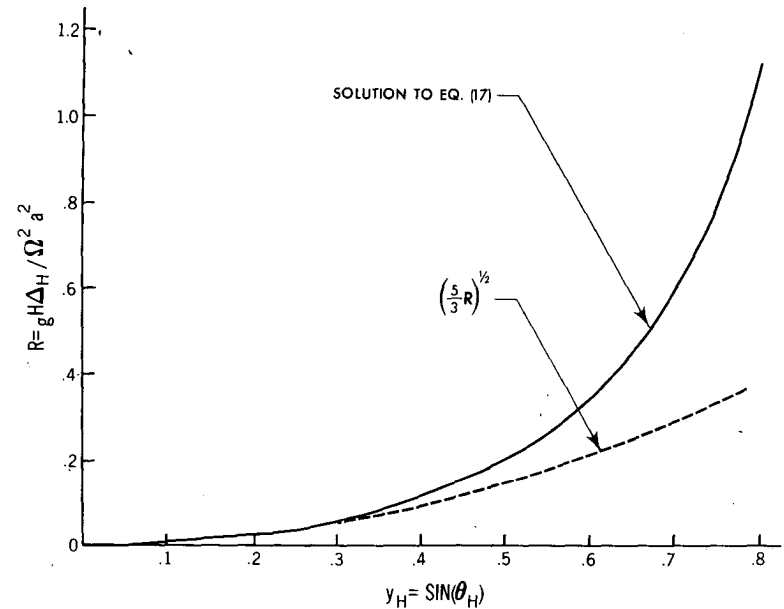


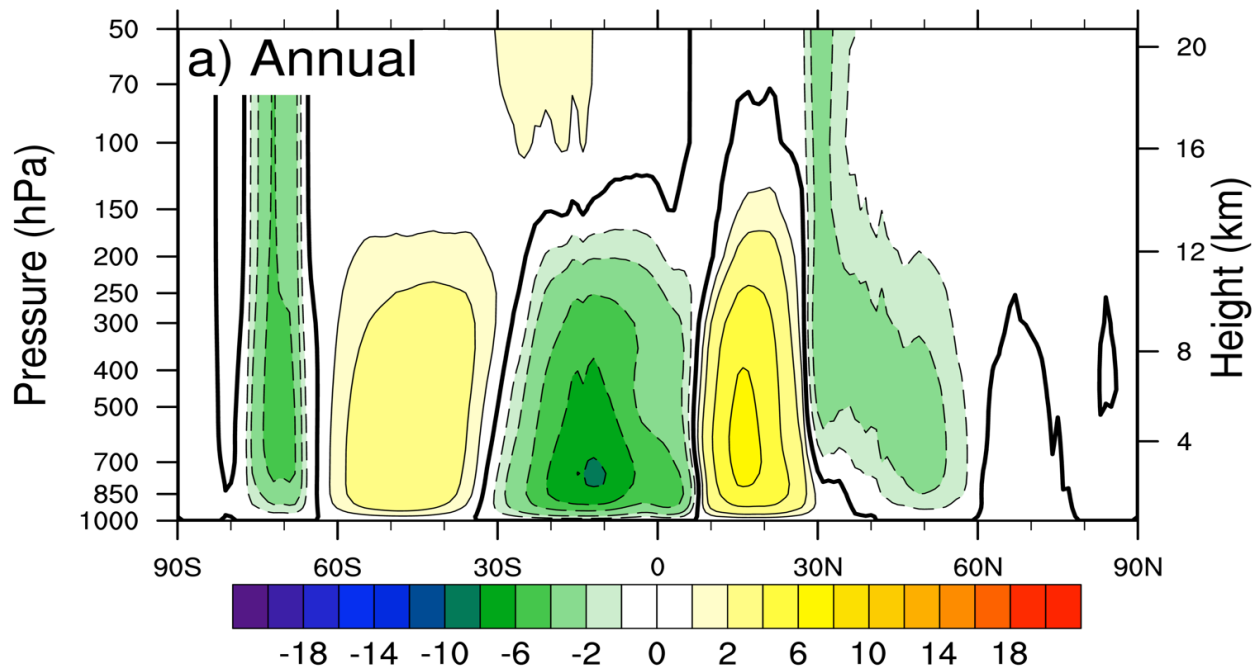
FIG. 2. The poleward boundary of the Hadley cell as given by (17) and the approximate solution $\Theta_H^2 = \frac{5}{3}R$ for $R \ll 1$.

Meridional mass flux stream function description of Hadley Circulation

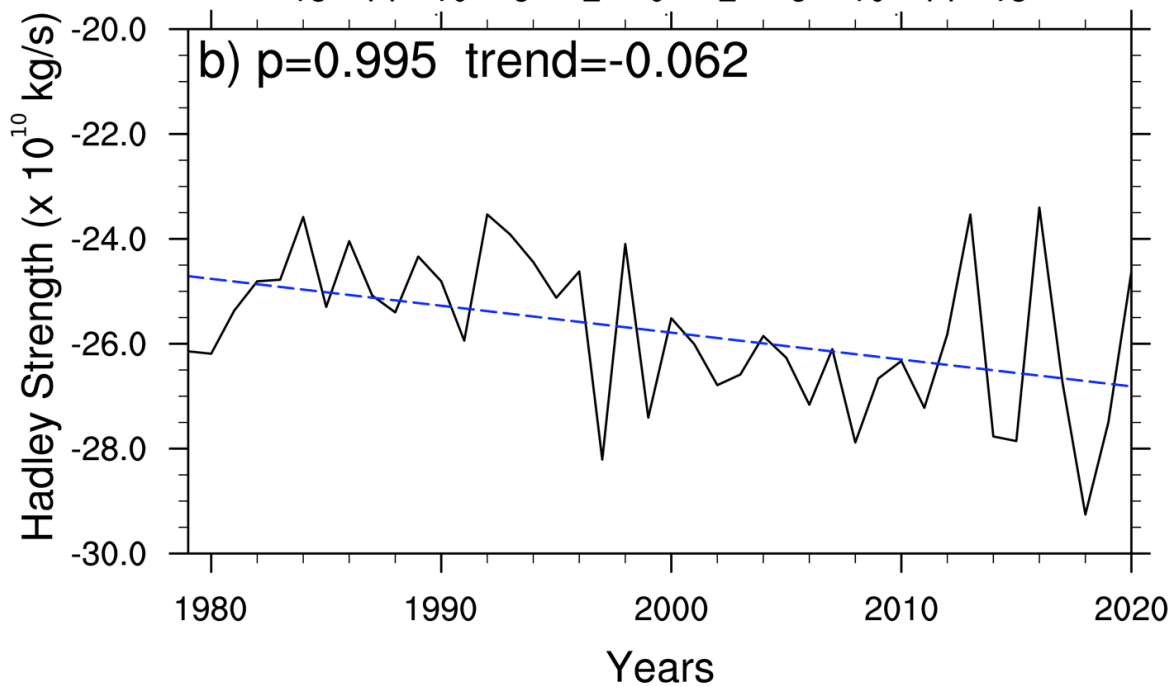
[11] The meridional stream function, Ψ , satisfying the zonal mean continuity equation in spherical coordinates can be calculated at each pressure, p , and latitude, φ , as a function of the downward integrated meridional wind, v , and is expressed as

$$\Psi(p, \varphi) = \frac{2\pi a \cos(\varphi)}{g} \int_p^{p_s} [v(p, \varphi)],$$

where a is the planetary radius, g is the gravitational acceleration, and bracketed terms denote a zonal average. Using this notation, v is by definition positive (i.e., northward) in regions where $-\partial\Psi/\partial z > 0$. Stream function values are set to zero at the top of the atmosphere, and the lowest level is modified such that Ψ equals zero at the lower boundary to ensure mass conservation and a steady state solution to the continuity equation.



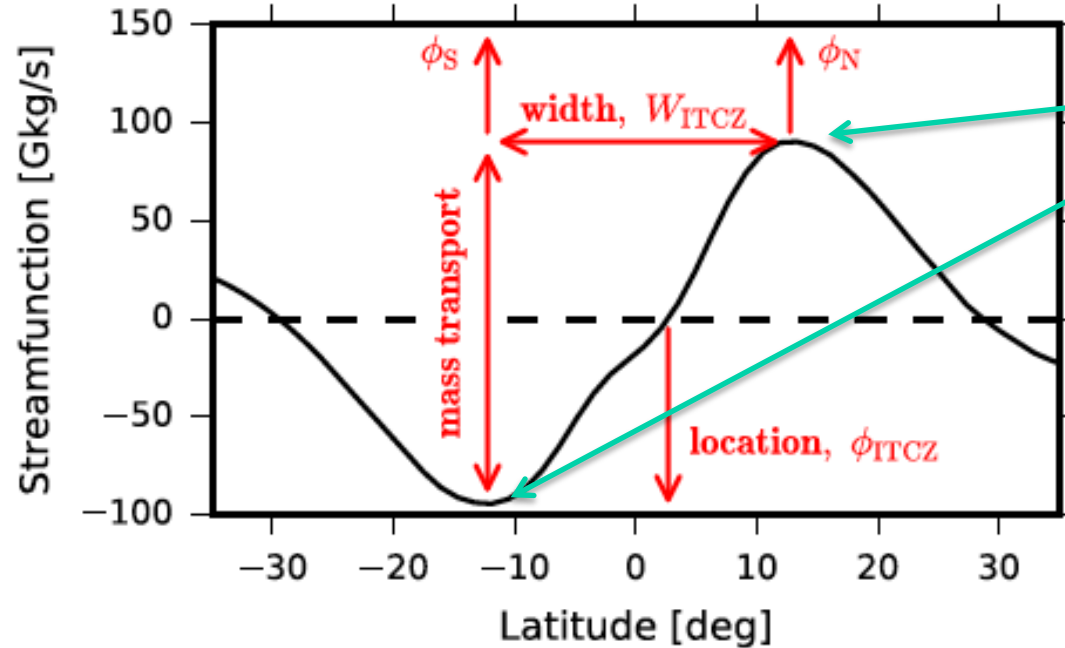
Climatological
annual mean
MMC from
NCEPv3
reanalysis
(1901-2015)



Trend of strength
of annual mean
Hadley circulation
as defined by
maximum Ψ from
ERA5 between
1979-2020.

An Alternative definition of ITCZ width using meridional stream function

Byrne et al., 2018: Current climate change reports



$$\partial\psi/\partial\phi = 0.$$

Vertically integrated annual and zonal mean meridional mass stream function (700-300 hPa mass weighted).

Location

$$\phi_{ITCZ} = \phi|_{\psi=0}.$$

Area

$$A_{ITCZ} = 2\pi a^2(\sin \phi_N - \sin \phi_S),$$

Width

$$W_{ITCZ} = \phi_N - \phi_S.$$

Intensity

$$\omega_{ITCZ} = -g\Psi_{ITCZ}/A_{ITCZ},$$

There is no standard definition of ‘width’ of the ITCZ or Hadley circulation. Another example.. (Byrne and Schneider, 2016, J. Climate)

$$\begin{aligned}\tilde{\omega}_i &\equiv \frac{\Psi(\sigma_L, \phi_0) - \Psi(\sigma_L, \phi_i)}{A_i} = \frac{-\Psi(\sigma_L, \phi_i)}{A_i}, \\ \tilde{\omega}_d &\equiv \frac{\Psi(\sigma_L, \phi_i) - \Psi(\sigma_L, \phi_t)}{A_d} = \frac{\Psi(\sigma_L, \phi_i)}{A_d},\end{aligned}\quad (1)$$

where Ψ is the Eulerian-mean streamfunction. From (1), the mass balance for the Hadley circulation can be written as

$$A_i \tilde{\omega}_i = -A_d \tilde{\omega}_d. \quad (2)$$

where

$$A_i = 2\pi R^2 (\sin\phi_i - \sin\phi_0),$$

$$A_d = 2\pi R^2 (\sin\phi_t - \sin\phi_i),$$

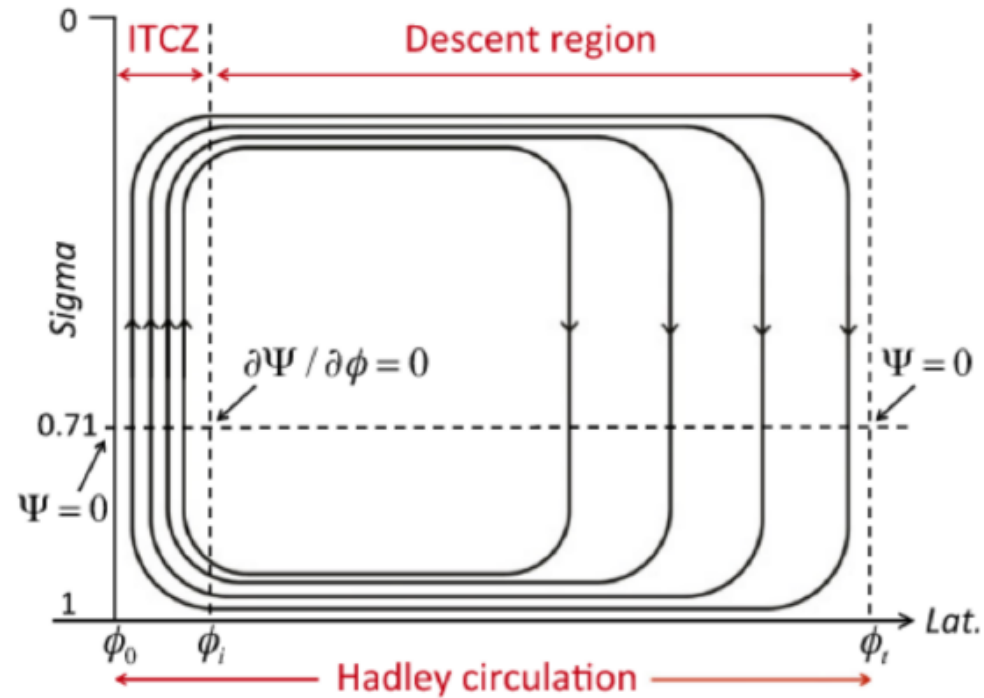


FIG. 2. Schematic diagram of the Hadley circulation with the boundaries of the ITCZ and the descent region indicated (following the definitions in section 2).

Dependence of the Width of the ITCZ on Global mean temperature (Global warming)

The width of the ITCZ is also being explained through energy constraints

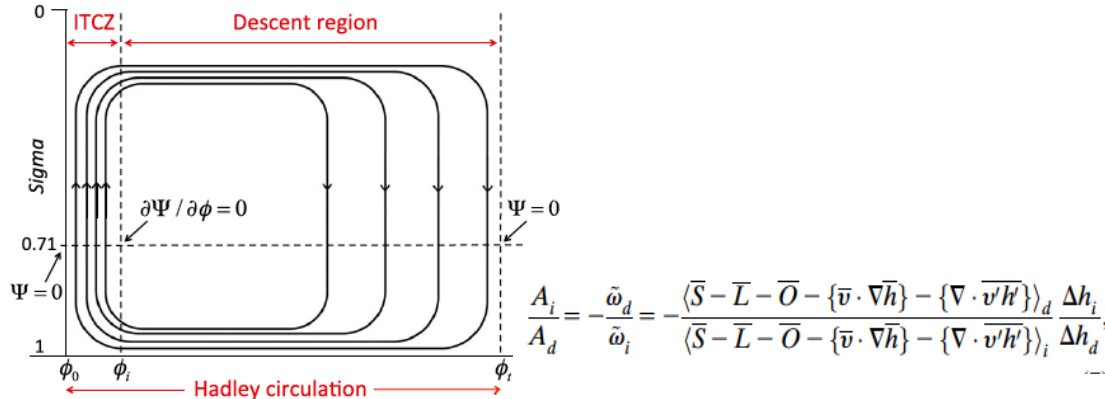


FIG. 2. Schematic diagram of the Hadley circulation with the boundaries of the ITCZ and the descent region indicated (following the definitions in section 2).

An idealized GCM forced by energy balance at TOA with infrared optical thickness $\tau = \alpha \tau_{\text{ref}}$

$\alpha = 0.4 \rightarrow T_{\text{gc}} = 269\text{K} \rightarrow \text{cold climate}$
 $\alpha = 1.0 \rightarrow T_{\text{gc}} = 286\text{K} \rightarrow \text{Earth like}$
 $\alpha = 6.0 \rightarrow T_{\text{gc}} = 314\text{K} \rightarrow \text{Hot climate}$

Byrne and Schneider, 2016

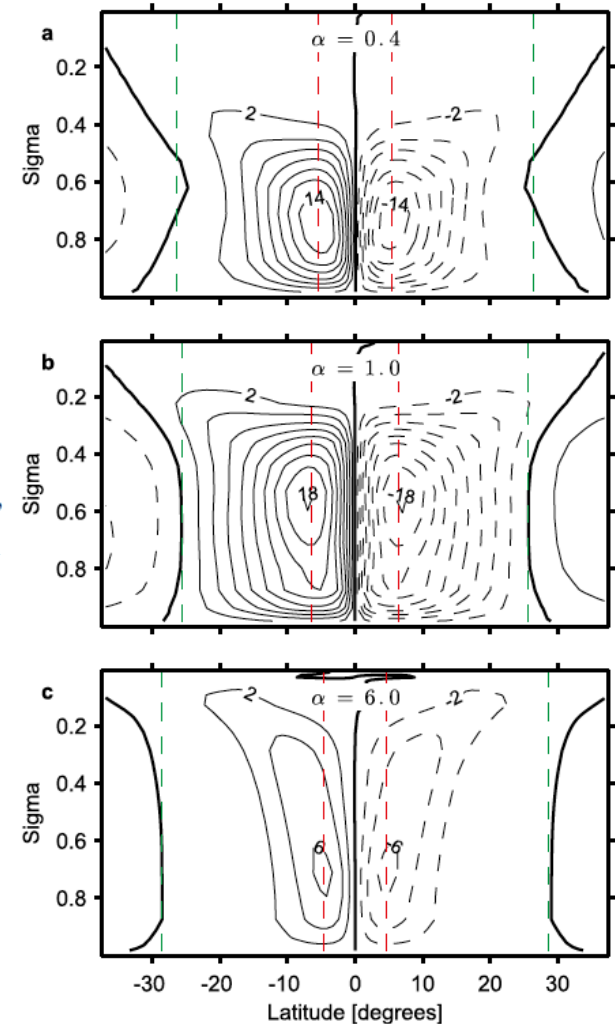


FIG. 3. Eulerian-mean streamfunction (time- and zonal-average) for (a) a cold simulation ($\alpha = 0.4$), (b) the reference simulation with a climate similar to that of the present-day Earth ($\alpha = 1.0$), and (c) a hot simulation ($\alpha = 6.0$). The contour interval is $2 \times 10^{10} \text{ kg s}^{-1}$. Dashed black lines denote negative streamfunction values and thick solid black lines denote the zero contours. The red and green dashed lines show the edges of the ITCZ and the descent region, respectively.

Width of the ITCZ vs width of the Hadley circulation

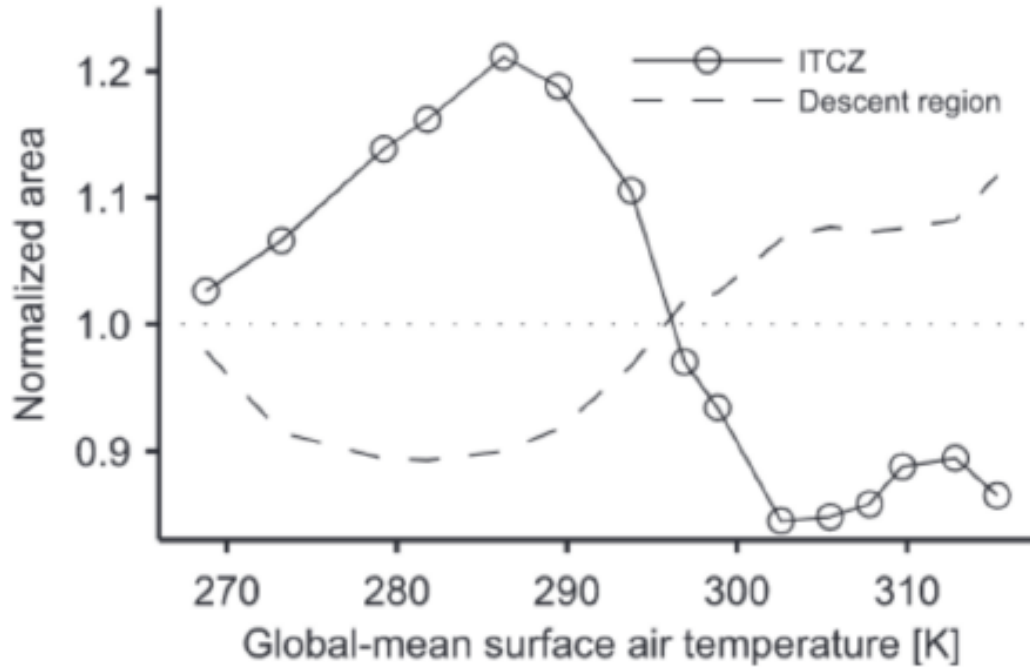
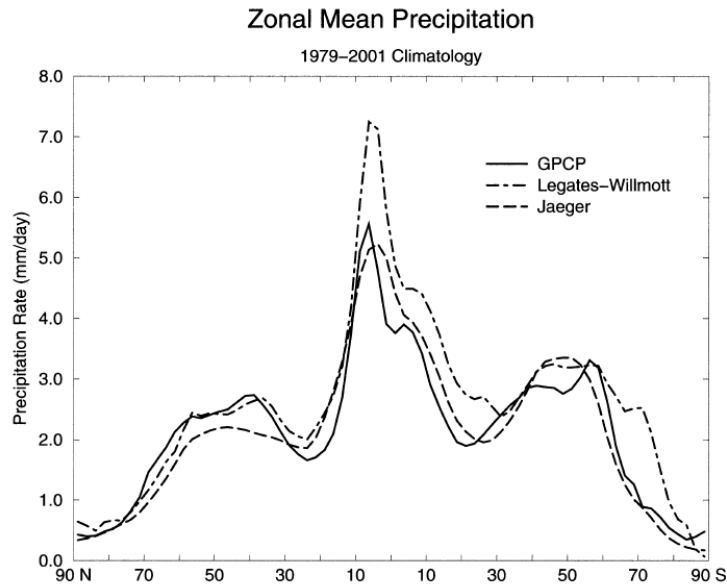


FIG. 5. Area of the ITCZ normalized by the ITCZ area averaged over all simulations (solid line), and descent region area normalized by the mean descent region area (dashed line) vs global-mean surface air temperature. Each dot represents a different simulation.

$\alpha = 0.4 \rightarrow T_{\text{sc}} = 269\text{K} \rightarrow \text{cold climate}$
 $\alpha = 1.0 \rightarrow T_{\text{sc}} = 286\text{K} \rightarrow \text{Earth like}$
 $\alpha = 6.0 \rightarrow T_{\text{sc}} = 314\text{K} \rightarrow \text{Hot climate}$
Byrne and Schneider, 2016

An idealized GCM forced by energy balance at TOA with infrared optical thickness $\tau = \alpha\tau_{\text{ref}}$

What determines the location of the ITCZ on annual mean and seasonal time scales?



Annual

Seasonal

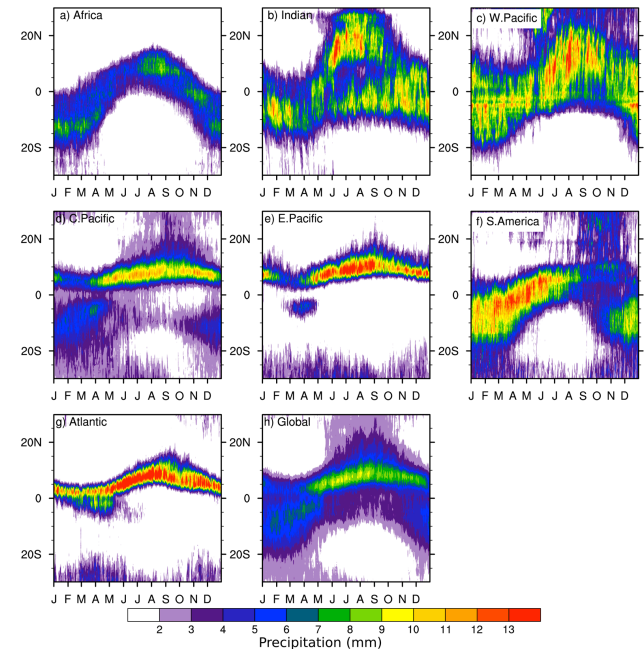


Fig. 5. Zonally averaged annual mean climatologies of precipitation (mm day^{-1}): the GPCP (solid line, see Fig. 4), Legates and Willmott (1990) (dot-dashed line), and Jaeger (1976) (long-dashed line).

For a long time we had no clear theory why the the ITCZ on annual mean is $\sim 6^\circ\text{N}$? Association with maximum of SST has been noted but does not provide a closed theory. Ocean-atmosphere interaction was proposed for the eastern Pacific (Xie and Philander, 1994, Tellus). Recently a theory based on Energy constraints has been proposed. We discuss the Energy constraint based theory.

Some Recent References:

(Energy Constraints on ITCZ Global monsoon and Hadley Circulation)

- Biasutti, M et al, 2018: Global energetics and local physics as drivers of past, present and future monsoons, *Nature Geoscience*, 392, 392–400
- Bischoff T and T. Schneider, 2014: Energetic Constraints on the Position of the Intertropical Convergence Zone, *J. Clim.*, DOI: 10.1175/JCLI-D-13-00650.1
- Bischoff T and T. Schneider, 2016: The Equatorial Energy Balance, ITCZ Position, and Double-ITCZ Bifurcations, *J. Climate*, Vol. 29, DOI: 10.1175/JCLI-D-15-0328.1
- Wei, H.-H., & Bordoni, S. (2018). Energetic constraints on the ITCZ position in idealized simulations with a seasonal cycle. *Journal of Advances in Modeling Earth Systems*, 10, 1708–1725. <https://doi.org/10.1029/2018MS001313>
- Ho-Hsuan Wei, Simona Bordoni, 2020: Energetic Constraints on the ITCZ position in the Observed Seasonal Cycle from MERRA-2 Reanalysis, *GRL*, doi: 10.1029/2020GL088506
- Schneider Tapio, Tobias Bischoff¹, & Gerald H. Haug, 2018: Migrations and dynamics of the intertropical convergence zone, *Nature*, 513, doi:10.1038/nature13636
- Byrne and Schneider, 2016: Energetic constraints on the width of the Intertropical Convergence Zone, *J. Climate*, 29, 4709
- Geen, Bordoni, Battisti & Hui, 2020: Monsoons, ITCZ & concept of Global Monsoon, *Rev Geophysics*

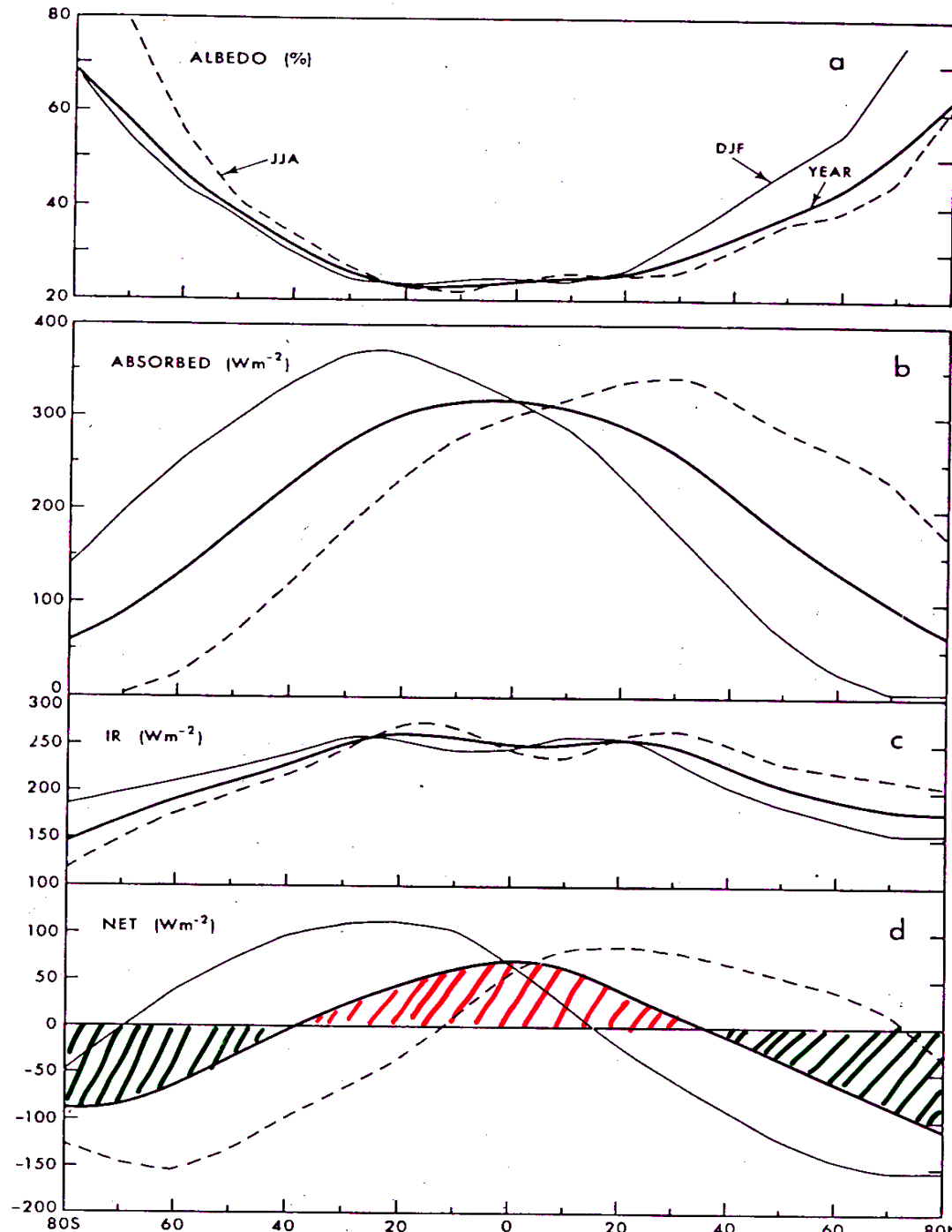
Recall the energy balance at top of atmosphere (right)

Excess heat balance in tropics → ascent

Deficit heat balance in polar region → descent

→ Hadley Circulation

→ Energy Constraint based Theory of ITCZ



Theory :

Atmospheric Energy Balance and Energy Transport

(Bischof and Schneider, 2014; J. Climate)

Zonal mean moist static energy equation integrated over the column is given by (Neelin and Held, 1987, MWR, 115)

$$S - \mathcal{L} - \mathcal{O} = \partial_y \langle \overline{vh} \rangle. \quad (1)$$

Where, $S \rightarrow$ net incoming SW radiation, $\mathcal{L} \rightarrow$ net outgoing LW radiation and $\mathcal{O} \rightarrow$ net energy uptake by the Ocean (at surface), $h \rightarrow$ moist static Energy.

At the ITCZ, low level winds converge and upper level winds diverge. Therefore, the location of the ITCZ and latitude δ at which the $(vh)_\delta$ changes sign (also called the Energy Flux Equator, EFE) must be close, if not identical.

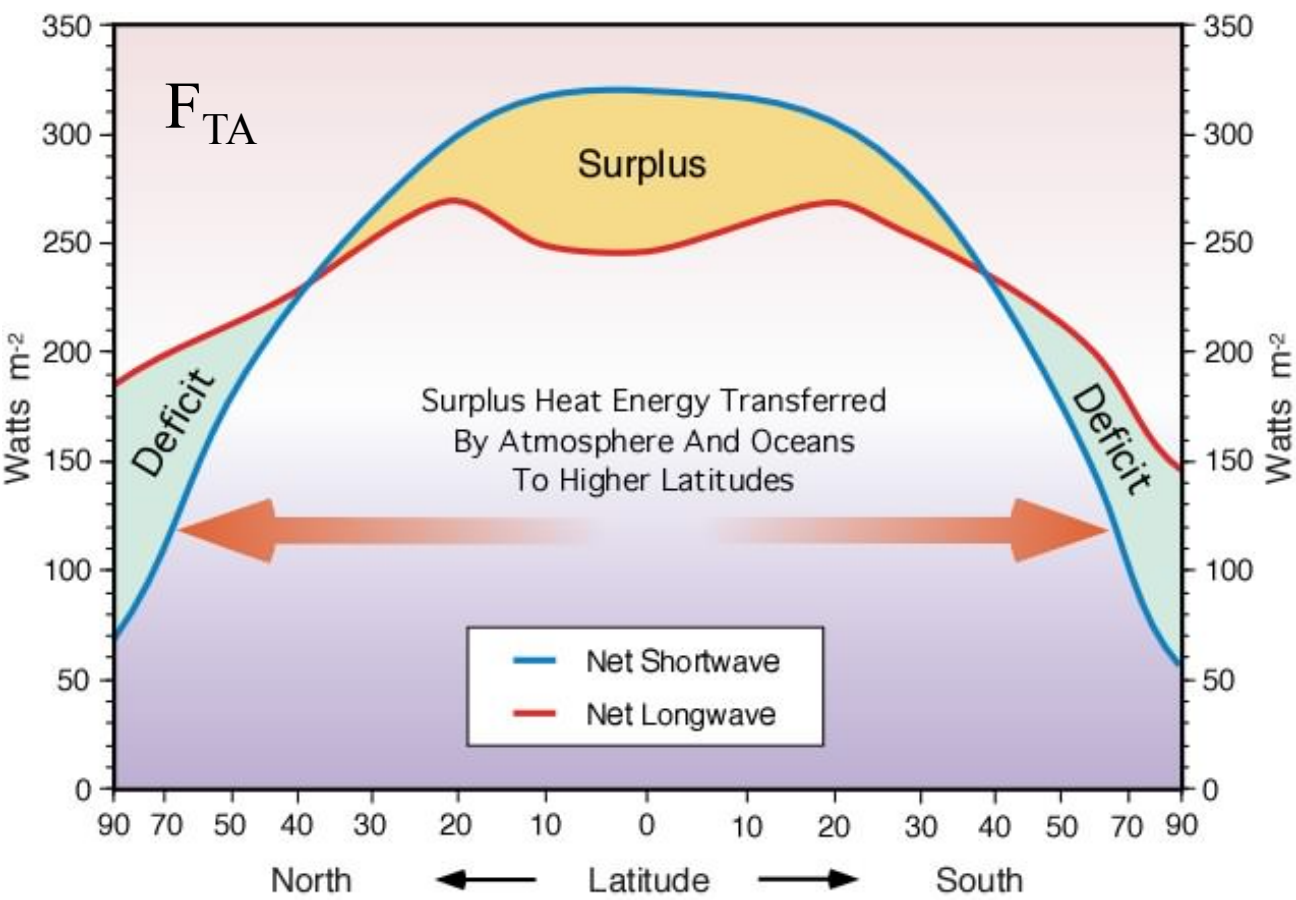
Expanding the atmospheric energy flux at low latitude δ around the equatorial flux, we obtain, **keeping only first order of δ terms,**

$$0 \approx \langle \overline{vh} \rangle_{\delta} = \langle \overline{vh} \rangle_0 + a \partial_y \langle \overline{vh} \rangle_0 \delta, \quad (2)$$

Where, subscript 0 denotes quantities evaluated at the equator. Solving for δ , we get the latitude location of the ITCZ as

$$\delta \approx -\frac{1}{a} \frac{\langle \overline{vh} \rangle_0}{S_0 - \mathcal{L}_0 - \mathcal{O}_0}. \quad (3)$$

This shows that the ITCZ position, to first order in δ , is proportional to the negative of the atmospheric energy flux across the equator $\langle \overline{vh} \rangle_0$, with the sensitivity of this dependence (the proportionality “constant,” which need not be constant) determined by the net energy input to the equatorial atmosphere $S_0 - \mathcal{L}_0 - \mathcal{O}_0$.² For Earth’s



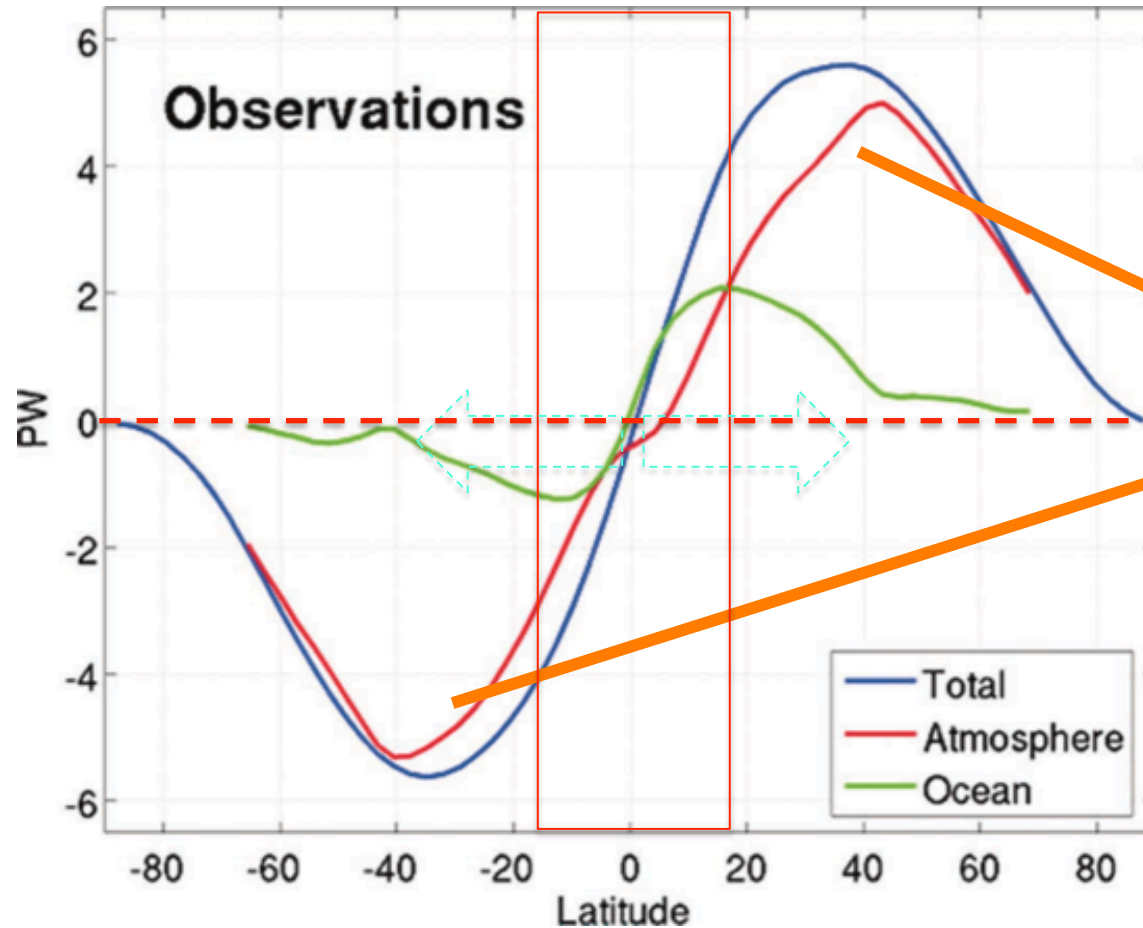
The net heat balance at the TOA also indicates that, for the earth's climate to be in equilibrium, there must be mechanisms in place that continuously transports heat from equatorial regions to the polar regions.

Required Heat Transport across latitude ϕ_1

$$T_A + T_O = - \int_{\phi_1}^{\pi/2} 2\pi r \cos \phi F_{TA} d\phi$$

Atmospheric transport \swarrow T_A \searrow T_O Oceanic transport

Required and observed energy transport across latitudes



Most of polewards transport of energy at extratropics is achieved by transient eddies (Weather)!

Black curve is the combined heat transport by the atmosphere and ocean; red, atmosphere heat transport (AHT); and blue, ocean heat transport (OHT). Units: PW; 1 PW = 10^{15} W. Each solid curve represents the mean heat transport during the LGM period (22–20 ka). Light color curve shows the spread of corresponding heat transport since the LGM. The data source is the CCSM3 TraCE-21K simulation. Dotted curves are the corresponding heat transports based on present-day observations¹

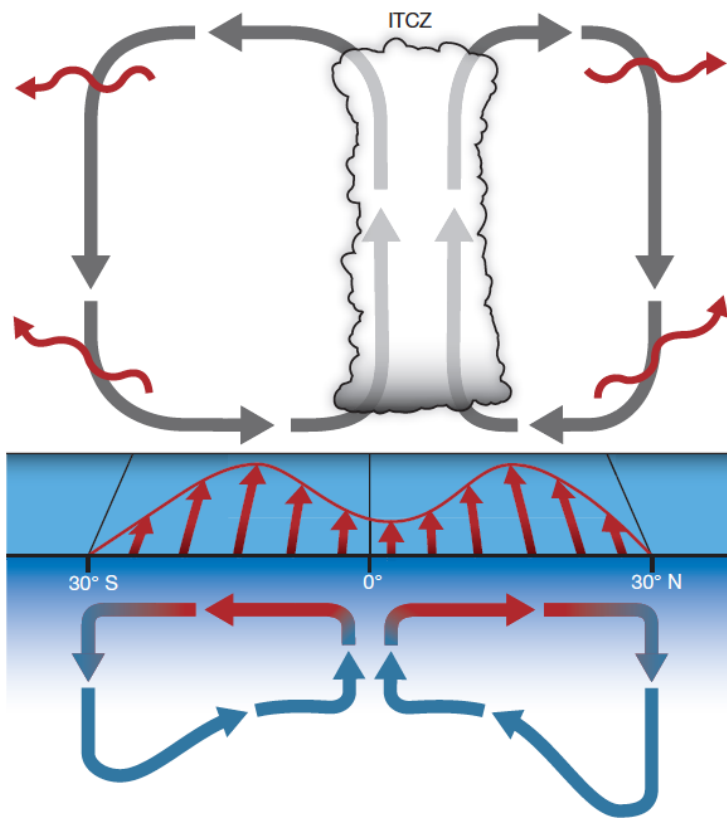


Figure 4 | Processes controlling zonal-mean ITCZ position. The lower branches of the Hadley circulation (grey arrows) bring warm and moist air masses towards the ITCZ, where they converge, rise and diverge as cooler and drier air masses aloft. Because the moist static energy aloft is greater than near the surface, the Hadley circulation transports energy away from the ITCZ. Eddies transport that energy farther into the extratropics (red wavy arrows). Hemispheric asymmetries in the energy export out of the tropics generally lead to an energy flux that crosses the Equator. Currently, the energy export into the extratropics in the south exceeds that in the north, leading to a southward cross-equatorial energy flux (Fig. 5). This implies an ITCZ in the Northern Hemisphere. Coupled to the Hadley circulation are mean zonal winds (red arrows at the sea surface), which are easterly where the near-surface mass flux is equatorward, and westerly where it is poleward. In the oceans, these zonal winds drive subtropical cells, with near-surface mass flux to the right of zonal winds in the Northern Hemisphere, and to the left in the Southern Hemisphere. Water masses cool and sink along their way towards the Hadley circulation termini and return below the sea surface (red and blue arrows). With mean easterlies in the tropics, the returning cool water masses upwell at the Equator, and the subtropical cells transport energy away from the Equator. But the upwelling location can migrate with the ITCZ away from the Equator and can dampen the ITCZ migration (Box 1).

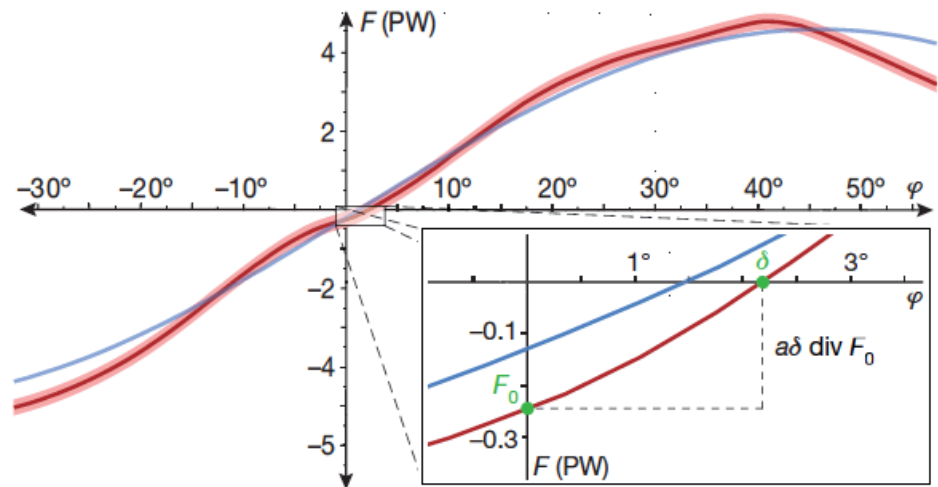
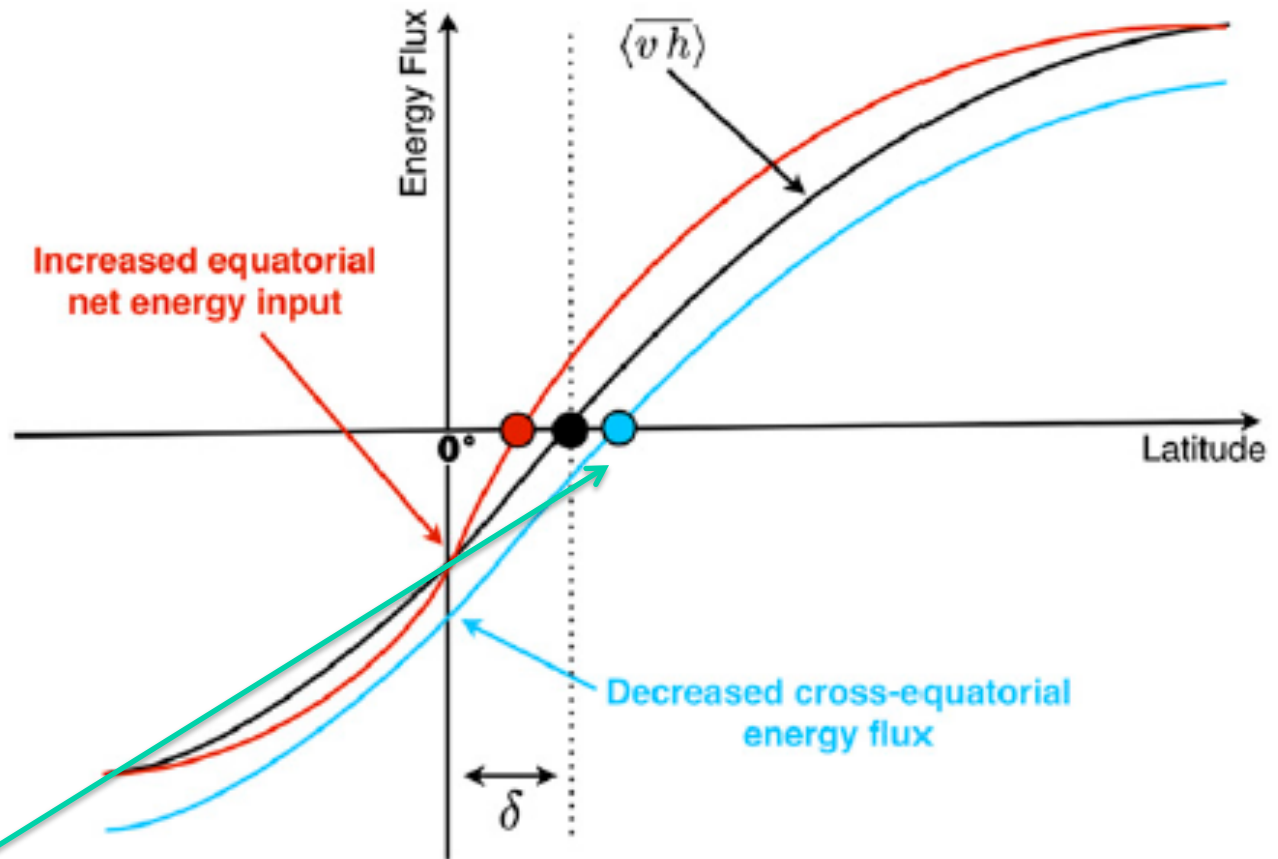


Figure 5 | Atmospheric meridional energy flux and energy flux equator. The atmospheric moist static energy flux F in the zonal and annual mean in the present climate (red line) is generally poleward, but it has a small southward component F_0 at the Equator. The energy flux equator is the zero of the energy flux, which currently lies around $\delta \approx 2.5^\circ$. Given the equatorial values of the energy flux F_0 and of its 'slope' with latitude $\text{div} F_0$, the energy flux equator δ can be determined from $F_0 \approx -a\delta \text{div} F_0$, where a is Earth's radius. For example, if F_0 increases (indicated schematically by the blue line), the energy flux equator δ moves southward. Similarly, if $\text{div} F_0$ increases, the energy flux equator moves towards the Equator. The energy flux data are from the ECMWF interim reanalysis for 1998–2012, corrected as in ref. 37 and provided by the National Center for Atmospheric Research. The light red shading indicates an estimated $\pm 0.2 \text{PW}$ standard error (the actual uncertainty is poorly known).

Schneider T. et al., 2014: Nature

Bischoff and
Schneider, 2014



Energy Flux
Equator (EFE)

FIG. 1. Qualitative behavior of the ITCZ position (large dots) as the northward cross-equatorial atmospheric energy flux $\langle \overline{v h} \rangle_0$ decreases (blue line) and as the net energy input to the equatorial atmosphere $S_0 - \mathcal{L}_0 - \mathcal{O}_0 = \partial_y \langle \overline{v h} \rangle_0$ increases (red line). Decreased northward energy flux at the equator shifts the zero of the energy flux and hence the ITCZ poleward. Increased energy input increases the divergence (slope) of the energy flux and shifts its zero and hence the ITCZ equatorward.

Aquaplanet model simulations support the EFE and MSE transport at equator and the Latitude of P_{ITCZ}

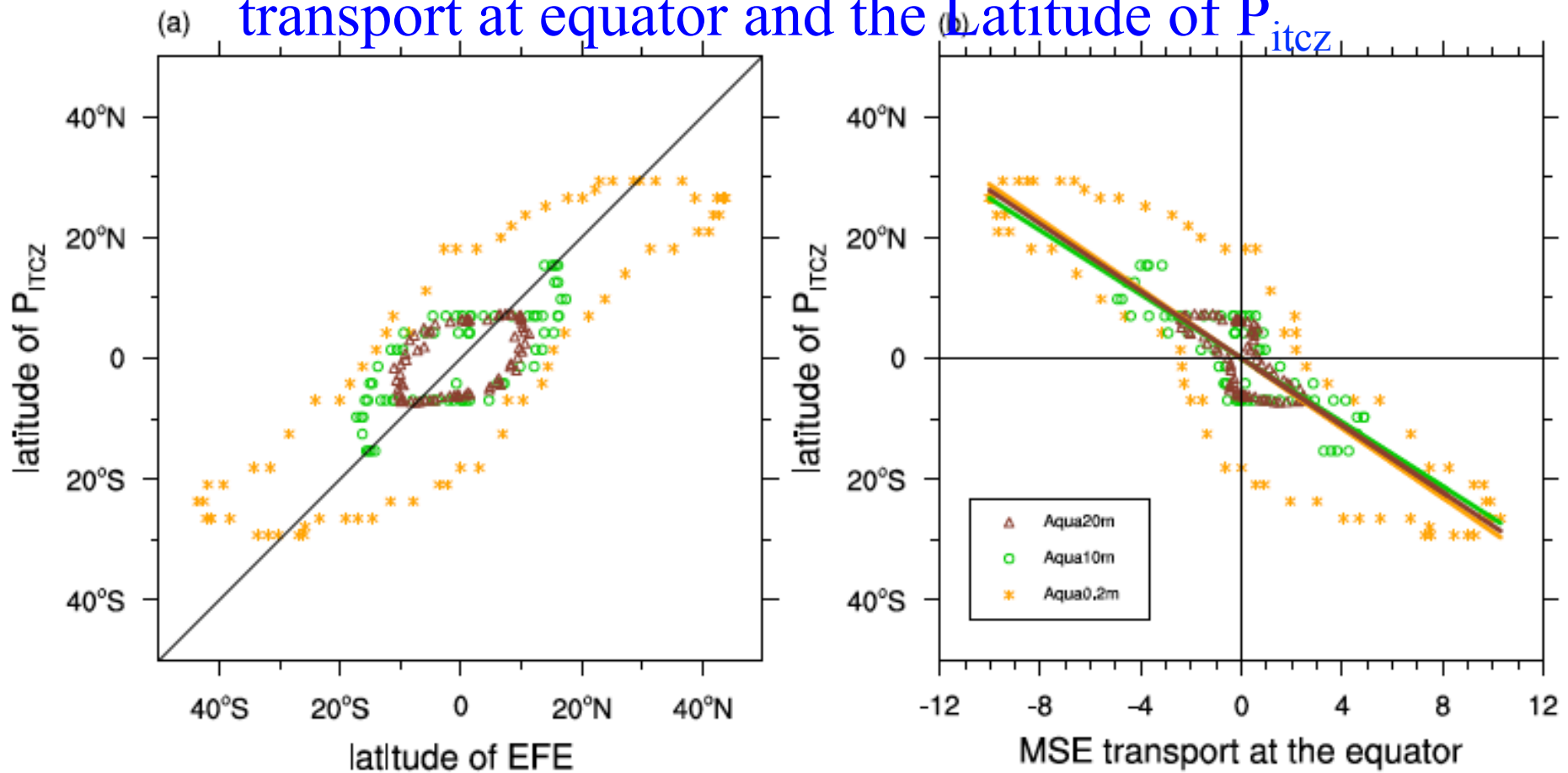


Figure 4. Scatter plot of the seasonal cycle of (a) $\phi_{P_{ITCZ}}$ versus $\phi_{EFE,actual}$ and (b) $\phi_{P_{ITCZ}}$ versus cross-equatorial energy transport in Aqua20m (brown open triangles), Aqua10m (green open circles), and Aqua0.2m (orange asterisks). The slopes in (b) are $-2.77^\circ/PW$ for Aqua20m, $-2.65^\circ/PW$ for Aqua10m, and $-2.87^\circ/PW$ for Aqua0.2m. ITCZ = intertropical convergence zone; MSE = moist static energy; EFE = energy flux equator.

However,

The energy flux and overturning circulation are related via the gross moist stability (GMS, defined here following e.g., D. M. W. Frierson, 2007; Hill, Ming, & Held, 2015; Wei & Bordoni, 2018, 2020):

Gross Moist Stability
$$GMS = \frac{\langle \overline{vh} \rangle}{\Psi_{max}} = \frac{\langle \overline{vh} \rangle}{g^{-1} \int_0^{p_m} \overline{v} dp}. \quad (14)$$

In the above, Ψ_{max} is the maximum of the overturning streamfunction, corresponding to the mass flux by the Hadley cell, and p_m is the pressure level at which this maximum occurs. Considering Eq. 14 at the Equator, and combining with Eq. 13, we see that the strength of the Hadley circulation (and hence the position of the convergence zone) will therefore covary with the EFE provided that the efficiency with which the Hadley cell transports energy, as captured by GMS, remains approximately constant. However, re-

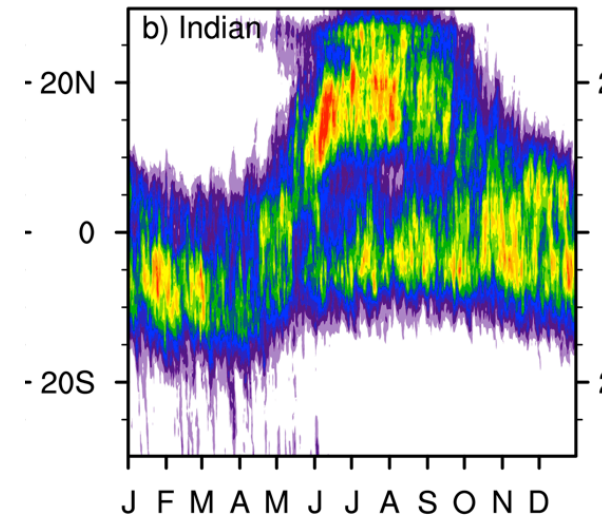
GMS could be influenced by

- Climate Change,
- Solar constant change due to astronomical factors

➔ The GMS must be factored in to interpret ITCZ location in the ‘Past’ as well as in ‘Future’.

Could the same Energy Constraints explain the position of Regional ITCZ like the the Indian summer Monsoon?

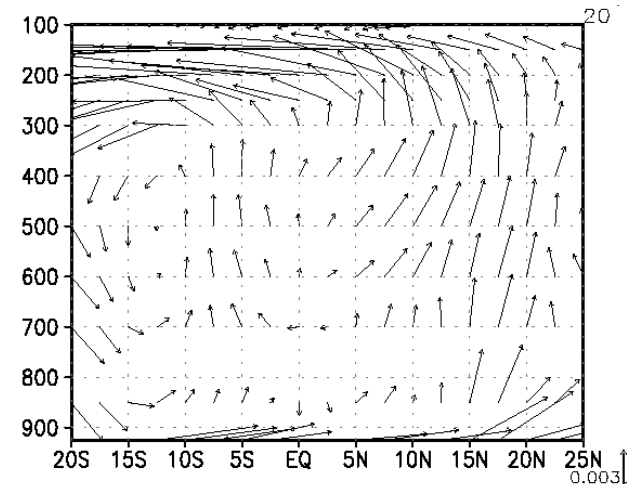
- **Indian monsoon ITCZ located $\sim 23^{\circ}\text{N}$**
- **It is seasonal, Boreal summer**
- **Monsoon Hadley circulation is ‘sector specific zonal mean’**



However,

The relationship between EFC and P_{ITCZ} , is based on

- **Annual mean, zonal mean MSE balance**



First, let us see how does the EFE and ϕ_{itecz} relationship work on 'global zonal mean Seasonal Cycle'

Wei and Bordoni, 2018, JAMES

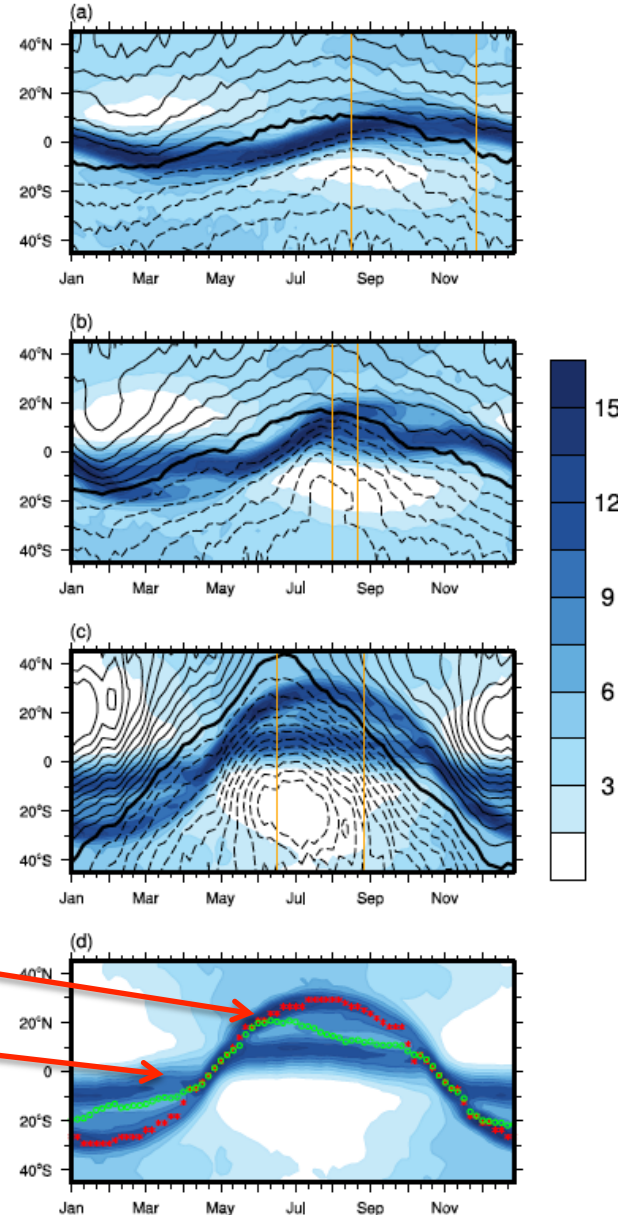
Idealized Aquaplanet with mixed layer Ocean, they introduce

$$\phi_{P_{\text{max,smth}}} = \frac{\int_{\phi_1}^{\phi_2} \phi [\cos\phi P]^N d\phi}{\int_{\phi_1}^{\phi_2} [\cos\phi P]^N d\phi}, \quad \phi_{P_{\text{max,smth}}}$$

Aqua20m

Aqua10m

Aqua0.2m



Red dots, $\rightarrow \Phi_{p_{\text{max}}}$

Blue thick line \rightarrow EFE

Green open circles $\rightarrow \phi_{P_{\text{max,smth}}}$

It is noted that,

The ITCZ always lags the EFE, even in the simulation with the shallowest mixed layer depth, making it possible for the EFE and the ITCZ to reside on opposite sides of the equator. At these times, which occur as the winter cross-equatorial Hadley circulation retreats from the summer hemisphere, the required energy balance is achieved not through shifts of the Hadley cell's ascending branch and ITCZ to track the EFE but through changes in the cell's vertical structure into one of negative **gross moist stability (GMS)**.

As land-ocean distribution, orography etc influence GMS, how applicable the results from idealized aquaplanet simulations are in observations.

Therefore, let us examine the potential relationship in observations (Reanalysis)

This is an area of active research currently

- Biasutti et al., 2018: Nature Geoscience
- Wei and Bordoni, 2020, GRL

Biasutti et al, 2018:
Nature Geoscience

Green line → ITCZ position
White patch → EFE
Shaded → Vertically
integrated energy flux

Indicates,
3° ITCZ shift per 1 PW
energy flux

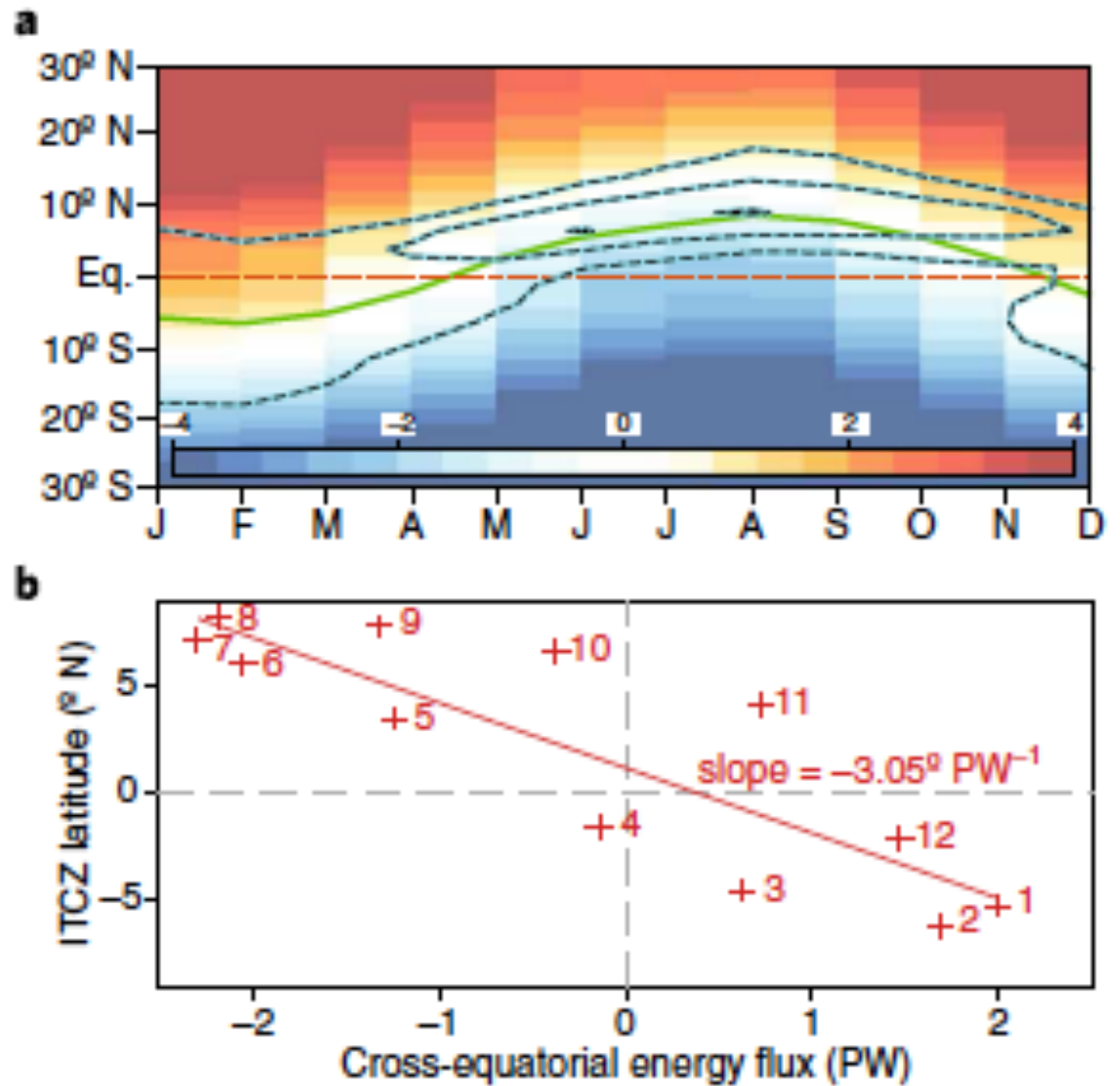


Fig. 3 | Rainfall in the ITCZ and in monsoons is linked to planetary and regional fluxes of energy. a, Zonal mean rainfall (dashed lines), ITCZ position (green line) and zonally and vertically integrated atmospheric energy transport (in PW, shaded). Letters on the x-axis represent the calendar month. **b**, Climatological ITCZ latitude as a function of the vertically integrated atmospheric energy transport at the equator. Numbers correspond to calendar month. The ellipse is sloped at 3° ITCZ shift per 1 PW energy flux. **c**, ITCZ (blue background) and monsoon (green background) schematics. The Hadley

Wei and Bordoni, 2020, GRL

Uses MERRA-2 Reanalysis data, 2002-2016

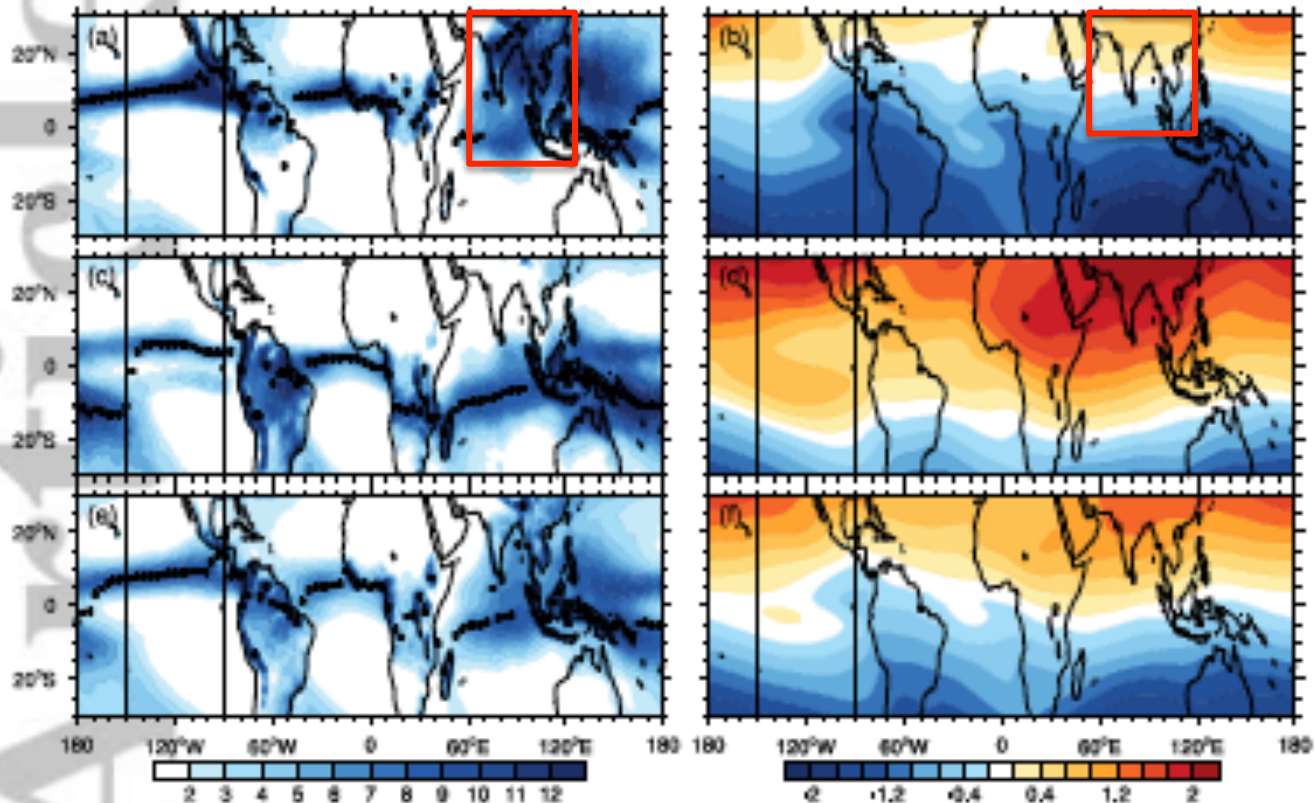


Figure 1. (a) JAS, (c) JFM, and (e) annual mean precipitation from MERRA-2 reanalysis data averaged over the years 2002–2016 (mm day^{-1}). Asterisks show the ITCZ position ($\phi_{P_{\text{max, annual}}}$; see Supplementary Information for further details on the specific ITCZ metric used). (b, d, f) Same seasonal mean as (a, c, e), but for the divergent component of the vertically integrated meridional MSE flux (10^8 W m^{-1}). The white shading represents where the meridional MSE flux vanishes, that is, the EFE. Black vertical lines indicate the Eastern Pacific sector.

Seasonal evolution of
 (a) zonal mean P and EFE
 while (b) MSE at lowest
 level ($\sigma = 0.985$)

Meridional stream
 function for two pentads
 around black lines in (a).
 Green line-EFE, blue line
 -ITCZ location

Note, bottom heavy
 Ψ makes the GMS
 negative during
 these times.

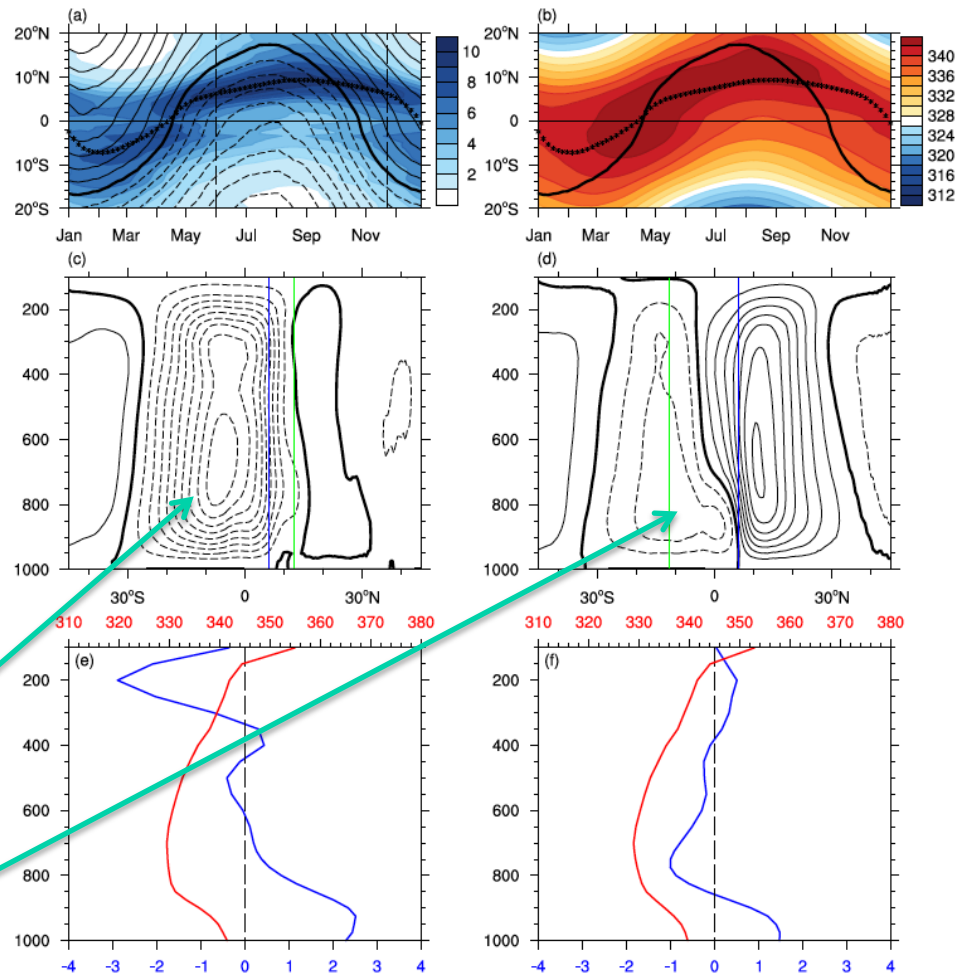


Figure 2. Seasonal evolution of (a) zonal mean precipitation (shading, mm day⁻¹) and vertically integrated meridional MSE flux (contours, W m⁻¹). Solid (dashed) contours indicate positive (negative) values and thick black contour the zero value (i.e., the EFE). The contour spacing is 2×10^7 W m⁻¹. Black vertical dashed lines indicate the two pentads used for panels (c)-(f). (b) Seasonal evolution of zonal mean MSE (K) at the lowest model level ($\sigma = 0.985$). The thick black contour indicates the EFE as in (a). The asterisks in (a, b) are the ITCZ location ($\phi_{P_{max, smth}}$). (c, d) Meridional mass streamfunction (contour, interval 2×10^{10} kg s⁻¹, positive (negative) value corresponding to clockwise (counter-clockwise) circulation) for (c) May 31–Jun. 4 and (d) Nov. 22–26. Solid (dashed) contours indicate positive (negative) values and thick black contours the zero value. Blue vertical line indicates the $\phi_{P_{max, smth}}$ and the green vertical line the location of the EFE. (e, f) Vertical profiles of the zonal mean MSE (red solid line, K) and meridional wind (blue dashed line, m s⁻¹) at the equator on (e) May 31–Jun. 4 and (f) Nov. 22–26.

$$\text{GMS} = \frac{\int_0^{P_s} [\overline{vh}] \frac{dp}{g}}{v_1}$$

Critique of the Energy constraint Theory of the ITCZ

- It is great concept but applicable Only for Annual Global Mean ITCZ or Global Monsoon!
- There are also difficulties in closing the MSE budget exactly from observations (or reanalysis) and suggest that conclusions based on energy constraints should be interpreted with caution.
- Even when ITCZ is defined on global zonal mean, clear offset exist between EFE and Φ_p during both Boreal summer and winter. Therefore, there are significant difficulty in applying the energy constraints to relate to seasonal location of the ITCZ

Challenges in applying to Indian monsoon ITCZ or Monsoon HC

- Even when ITCZ is defined on global zonal mean, clear offset exist between EFC and Φ_p during both Boreal summer and winter.
- Therefore, it is unclear how the energy constraint could be applied to Indian monsoon ITCZ or monsoon Hadley circulation which is a sectorial zonal mean seasonal Hadley circulation!
- Is it possible to close MSE budget for the sectorial mean? Unless that could be done, we may not be able to use the concept for Indian monsoon ITCZ.
- However, the Monsoon HC is quite strong and contributes to MSE transports within the sector. In the IO too, the shallow MMC contributes to transports of considerable energy. Together, could they lead to some sort of MSE closure over the sector?

Thank You

Wei and Bordoni, 2018,
JAMES

Simulated the **Summertime**
ITCZ in an Aqua Planet with
a mixed layer ocean with
mixed layer of 20m
(Aqua20m), 10m
(Aqua10m) and 0.2m
(Aqua0.2m) respectively.

EFE \rightarrow Energy flux equator

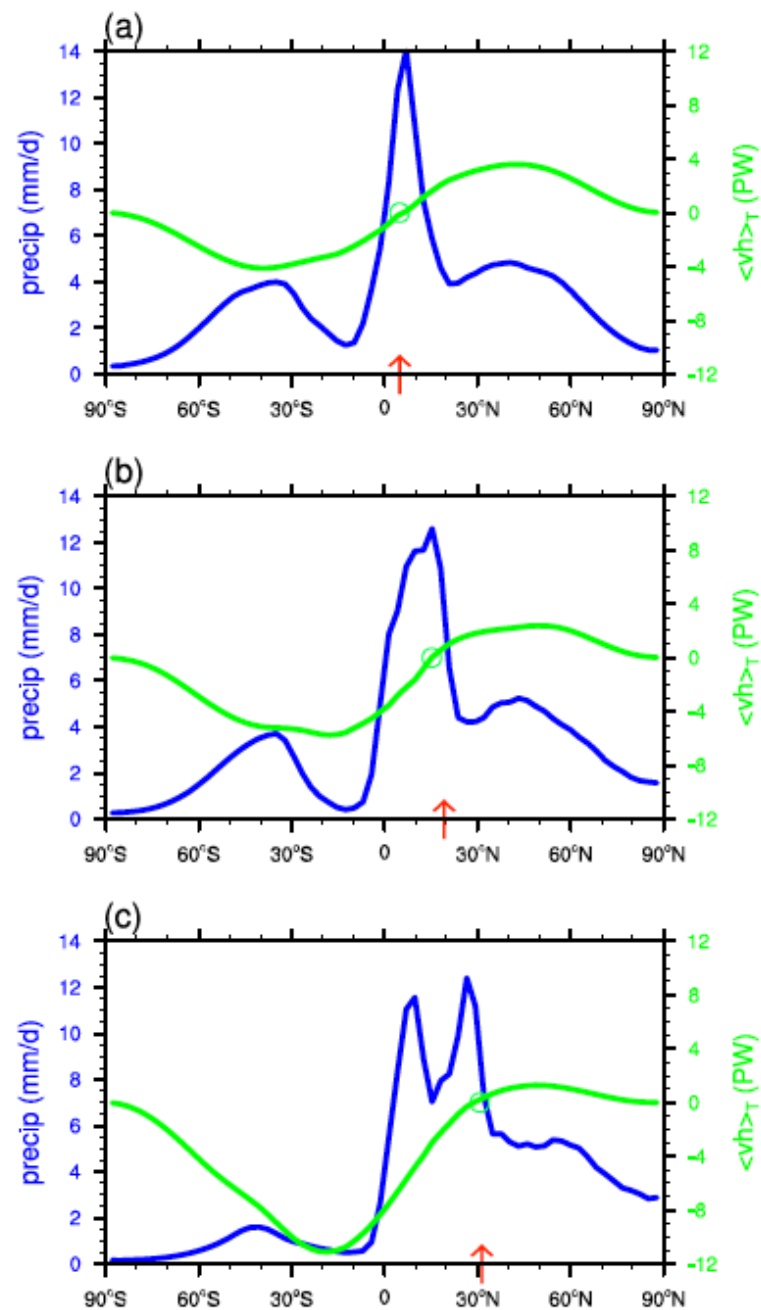


Figure 3. Summertime zonal mean precipitation (blue) and vertically integrated energy transport (green) in (a) Aqua20m, (b) Aqua10m, and (c) Aqua0.2m. The green circles are $\phi_{EFE,actual}$ and the red arrows $\phi_{EFE,analytical}$.

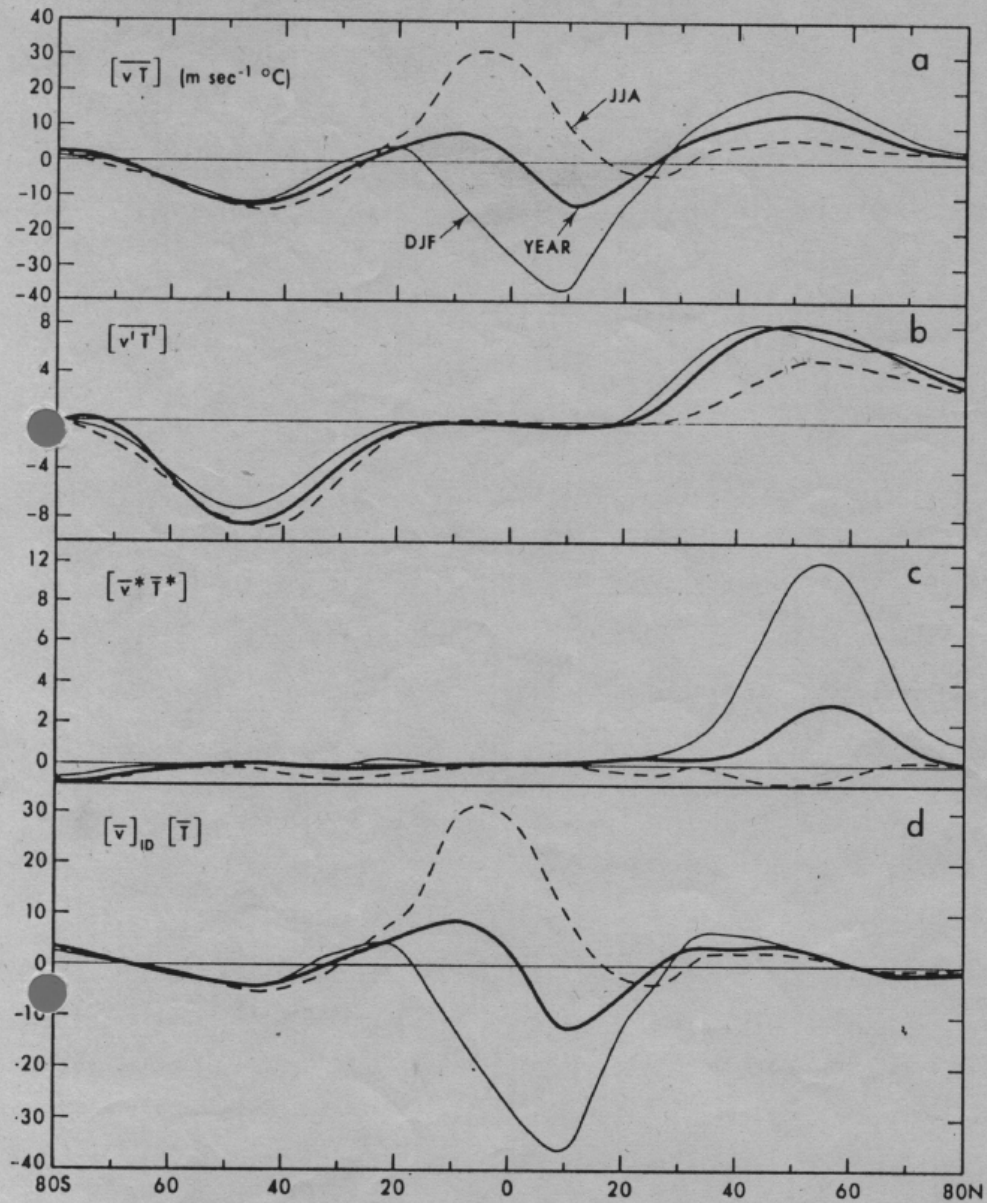
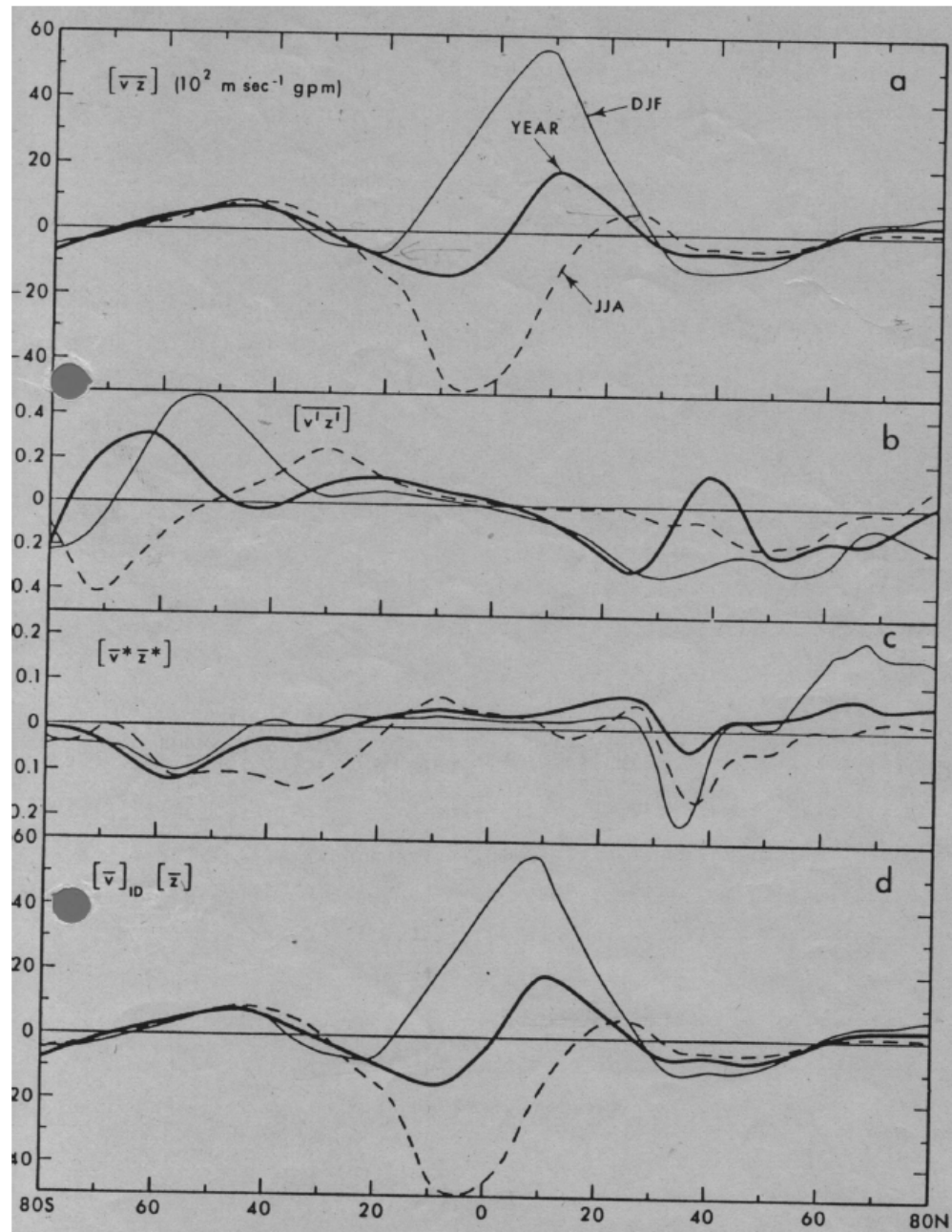


FIG. 30. Meridional profiles of the zonal and vertical mean northward flux of sensible heat (a) all motions, (b) transient eddies, (c) stationary eddies, and (d) mean meridional circulations for the 10-yr period.



32. Meridional profiles of the zonal and vertical mean northward transport of energy by (a) all motions, (b) transient eddies, (c) stationary eddies, and (d) mean zonal circulations.

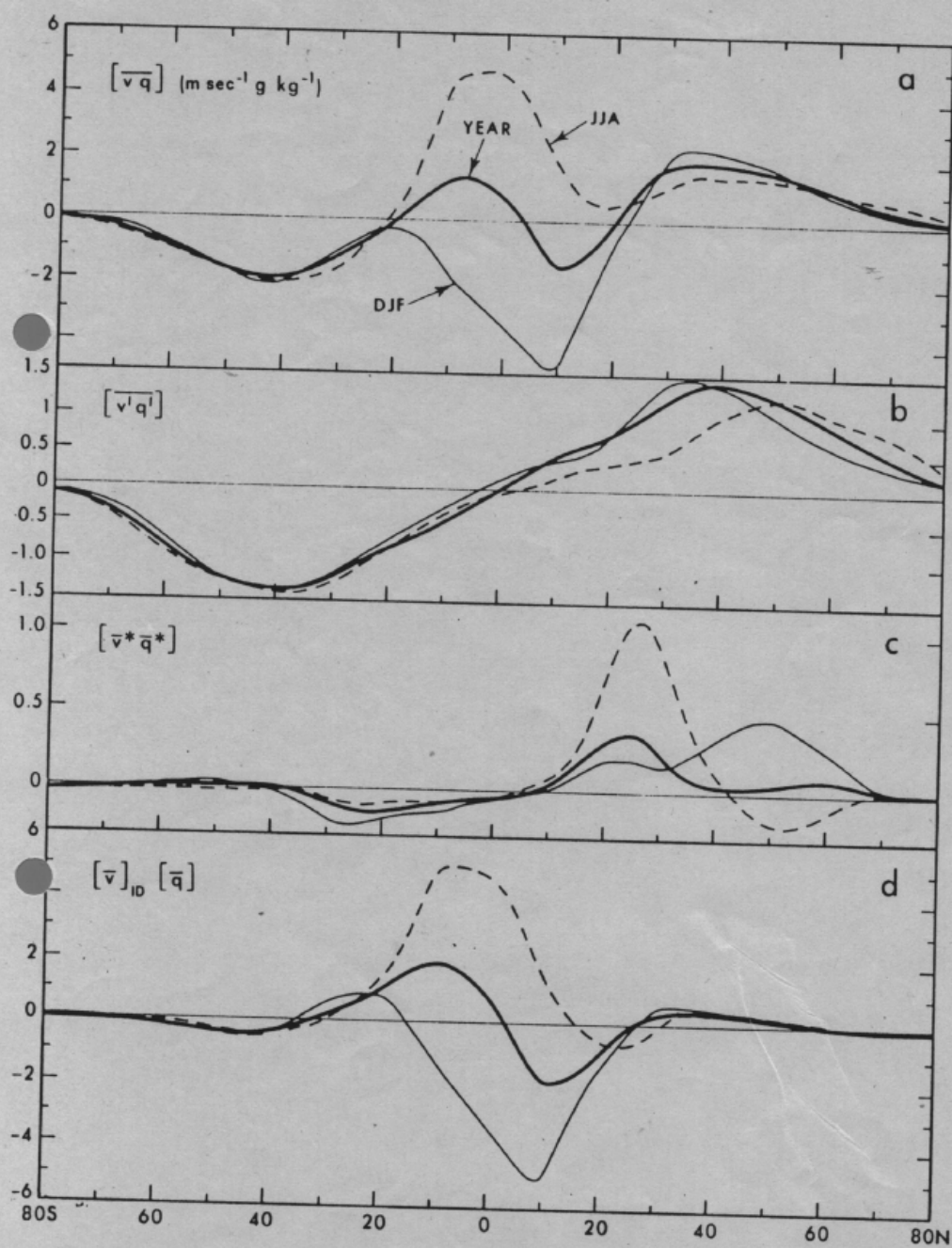


FIG. 35. Meridional profiles of the zonal and vertical mean northward transport of specific humidity by (a) all motions, (b) transient eddies, (c) stationary eddies, and (d) mean meridional circulations.

Energy in Atmosphere

$$E = c_v T + gZ + Lq + \frac{1}{2}(u^2 + v^2)$$

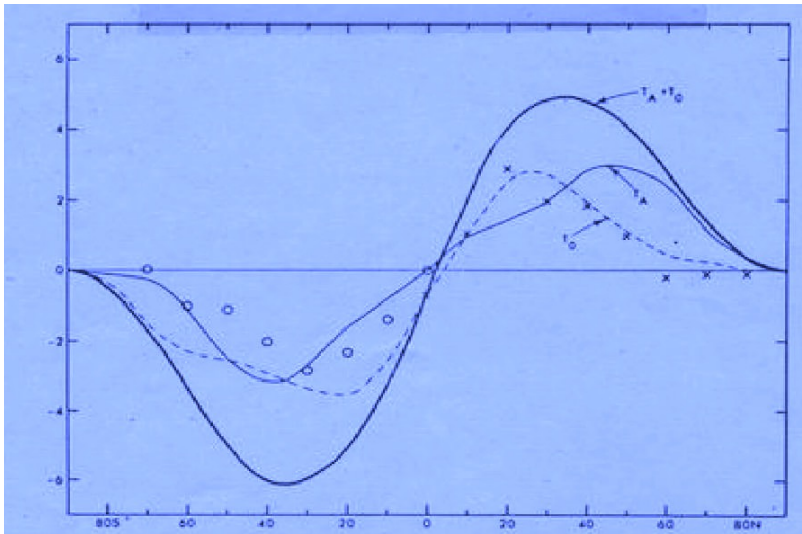


FIG. 46. Meridional profiles of the northward transports of energy in the atmosphere, oceans, and atmosphere plus oceans for annual mean conditions. Added are earlier estimates by Oort and Vonder Haar (1976) (x) and Trenberth (1979) (o).

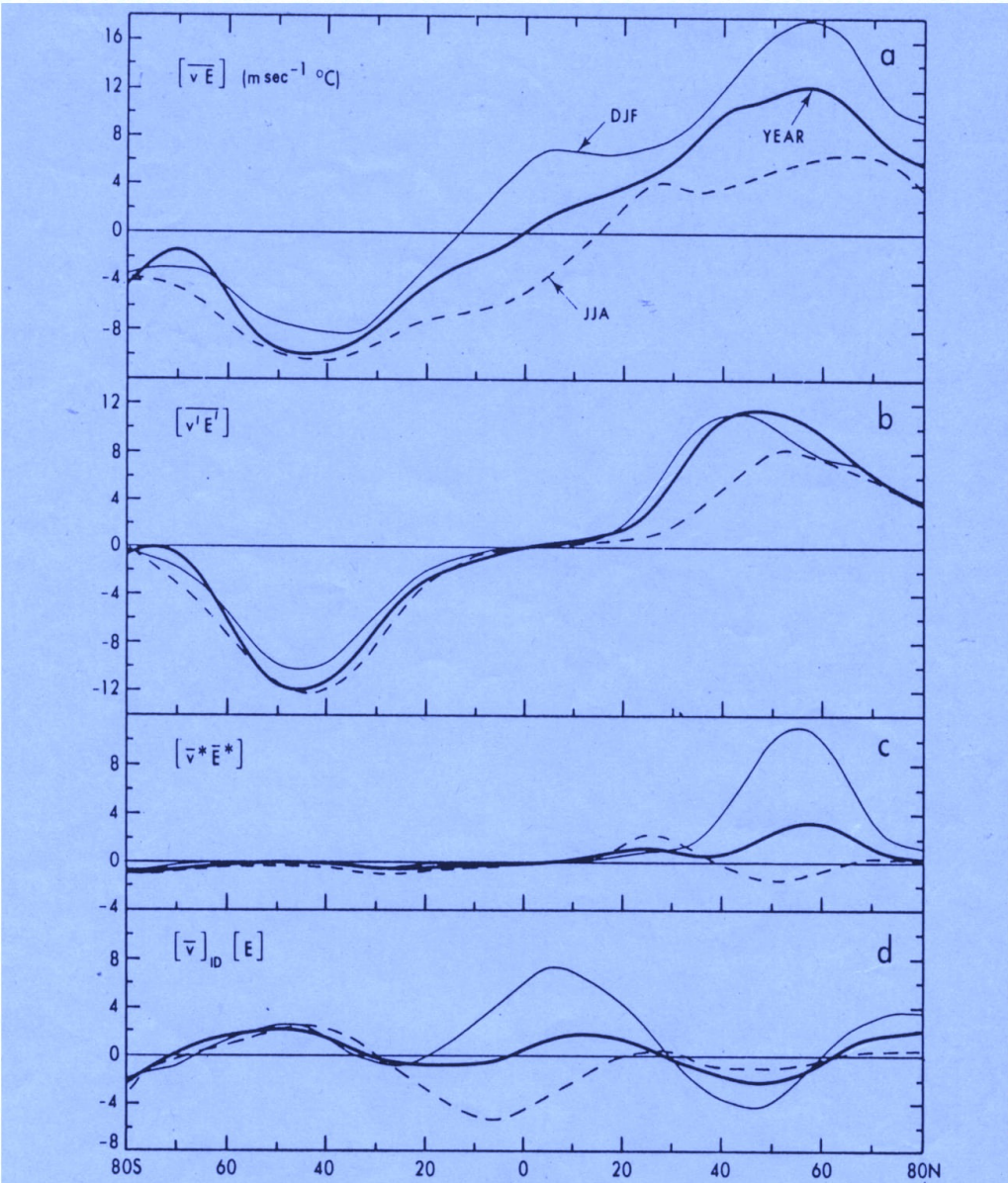


FIG. 39. Meridional profiles of the zonal and vertical mean northward transport of total energy by (a) all motions, (b) transient eddies, (c) stationary eddies, and (d) mean meridional circulations.

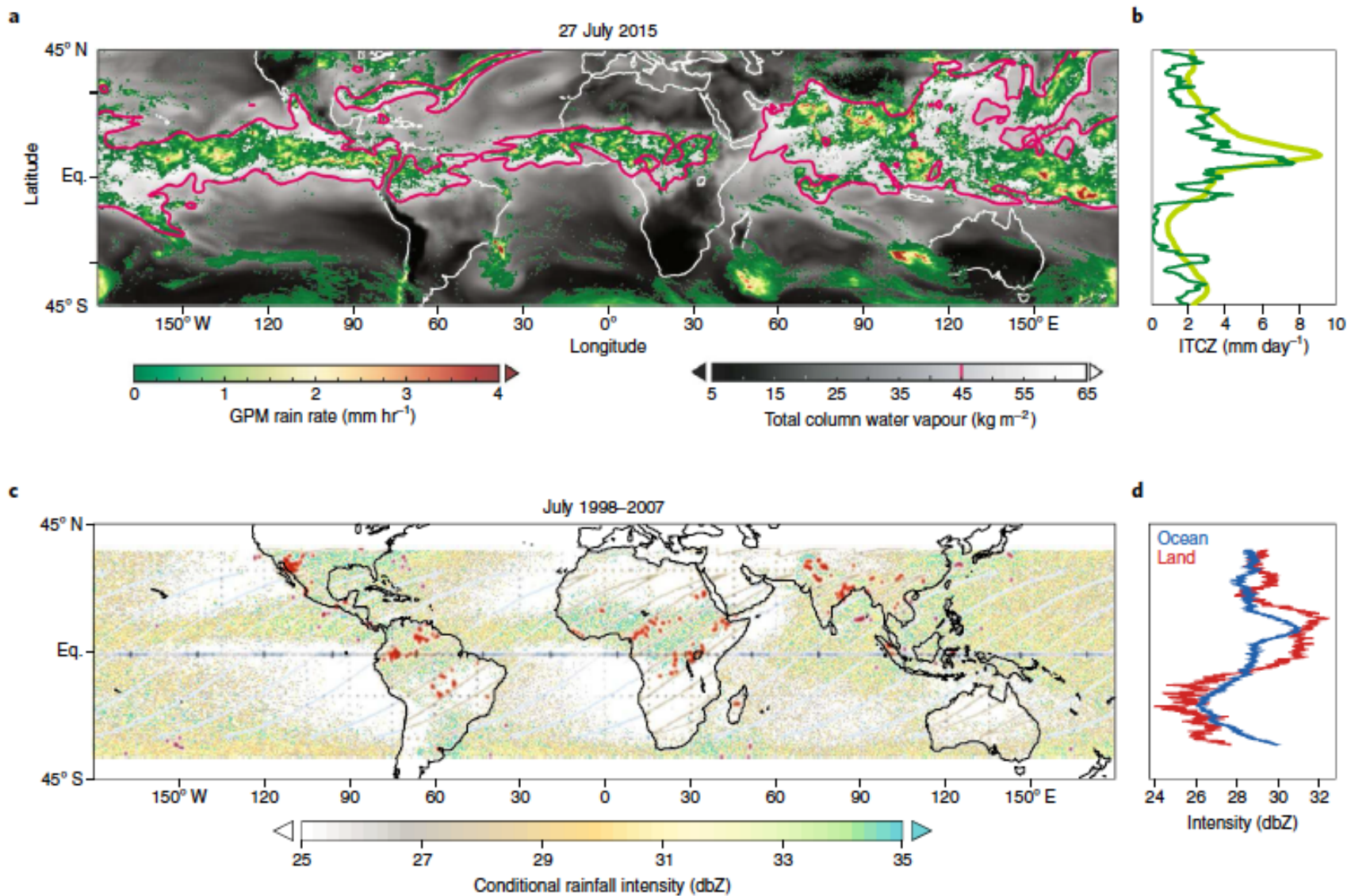


Fig. 1 | Distinct tropical convection systems are organized in a planetary-scale rain belt. a, Rainfall (coloured) on 27 July 2015, and the high atmospheric moisture enveloping it (indicated by the 45 mm contour of column-integrated water vapour, the full field is in grey). GPM, global precipitation measurement. **b**, Zonal mean rainfall for the same day (dark green) and climatological values for the same period (light green). **c**, July climatological mean intensity of instantaneous near-surface rainfall (from the Tropical Rainfall Measuring Mission (TRMM) precipitation radar, units of reflectivity (dBZ)) and occurrence of lightning (red dots) on 27 July 2014 (ascending passes of the lightning imaging sensor on TRMM). **d**, Zonal mean rainfall intensity for ocean (blue) and land (red) regions. See Methods for further details.